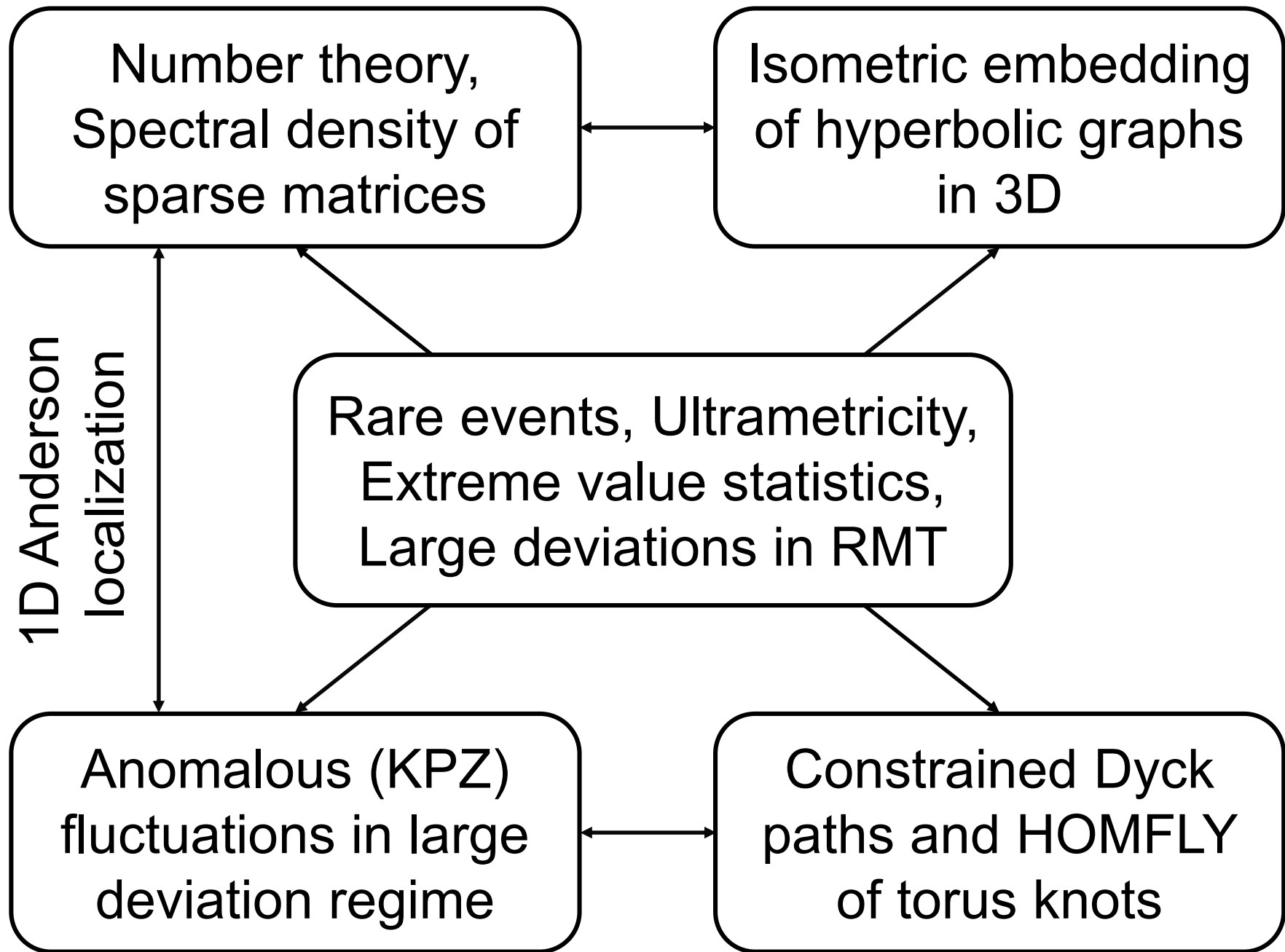
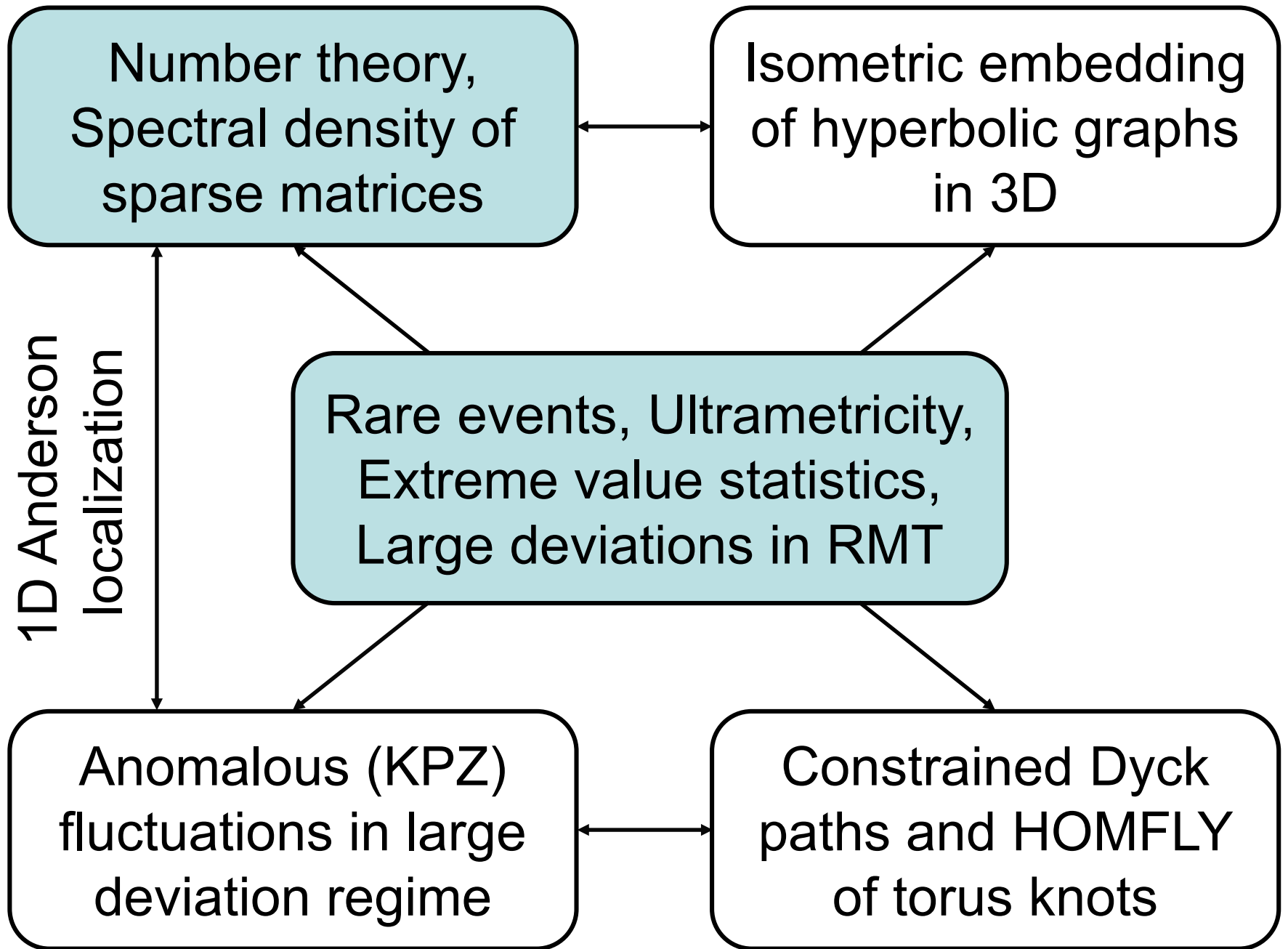


Rare event statistics ... and beyond

Sergei Nechaev

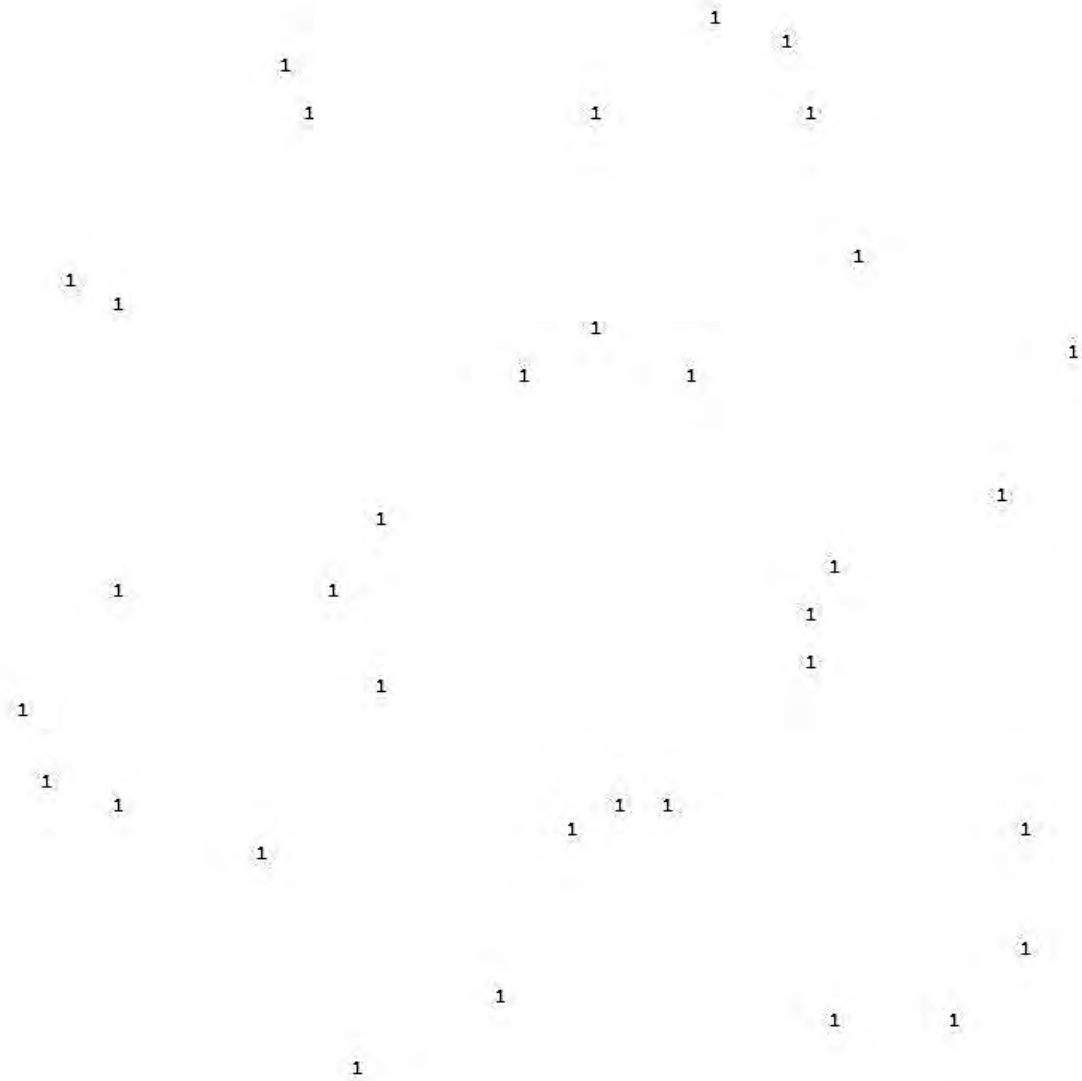
*Interdisciplinary Scientific Center Poncelet,
CNRS, Moscow*





$$a_{ij} = \begin{cases} 1 & \text{prob } r \\ 0 & \text{prob } 1-r \end{cases}$$

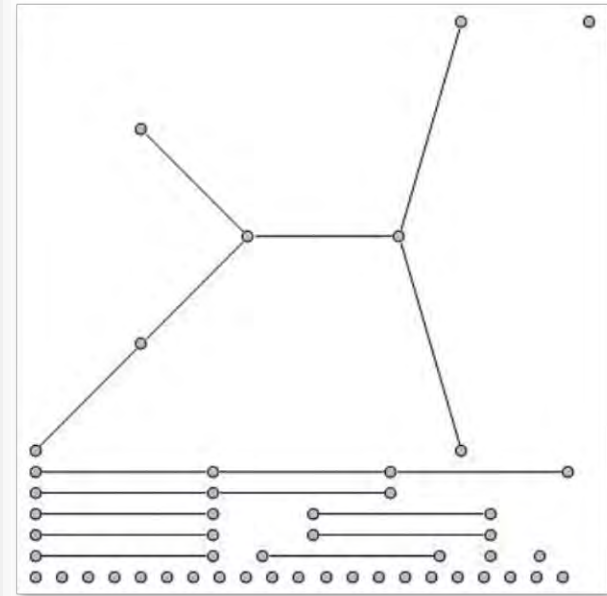
$$N \times N = 50 \times 50$$



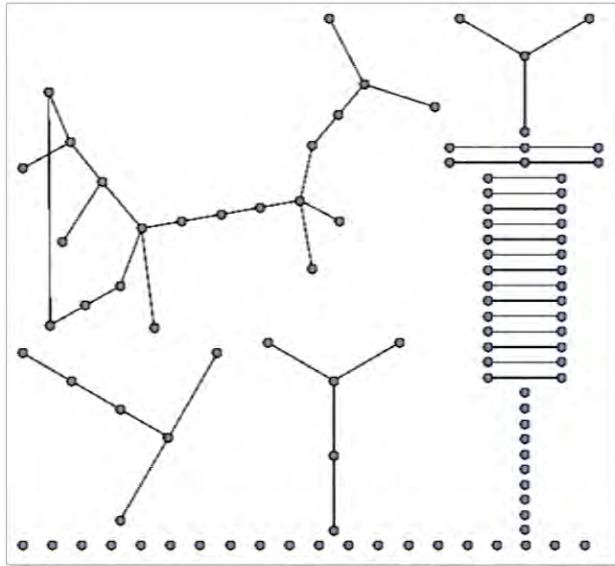
$r = \frac{1}{N}$, corresponds to percolation ($N \gg 1$)

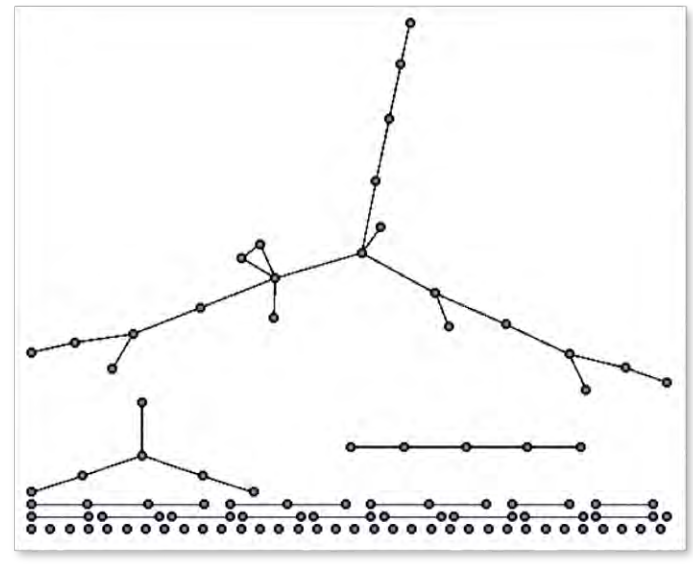
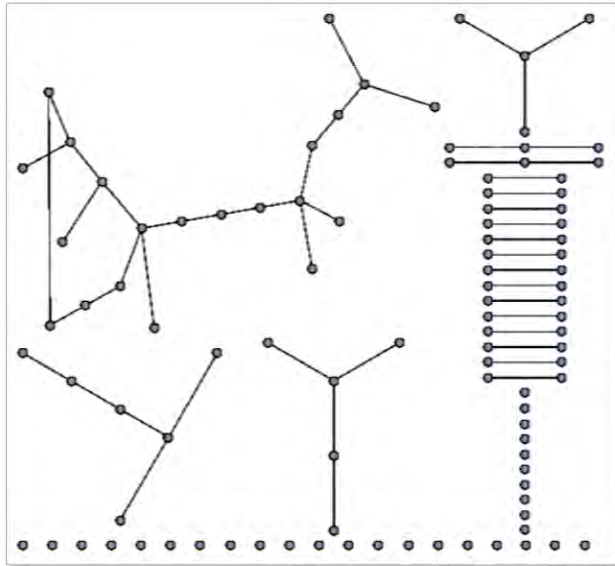
$$a_{ij} = \begin{cases} 1 & \text{prob } r \\ 0 & \text{prob } 1-r \end{cases}$$

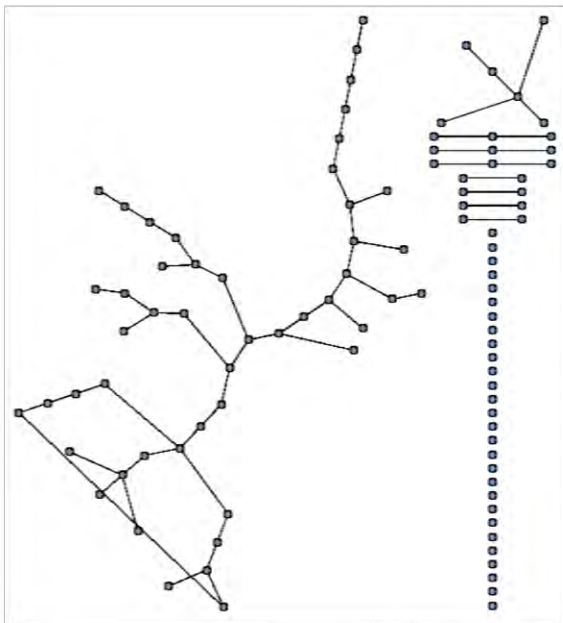
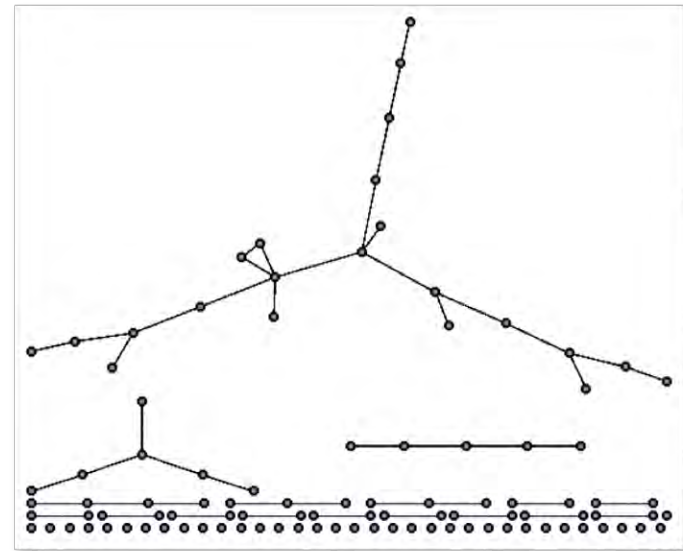
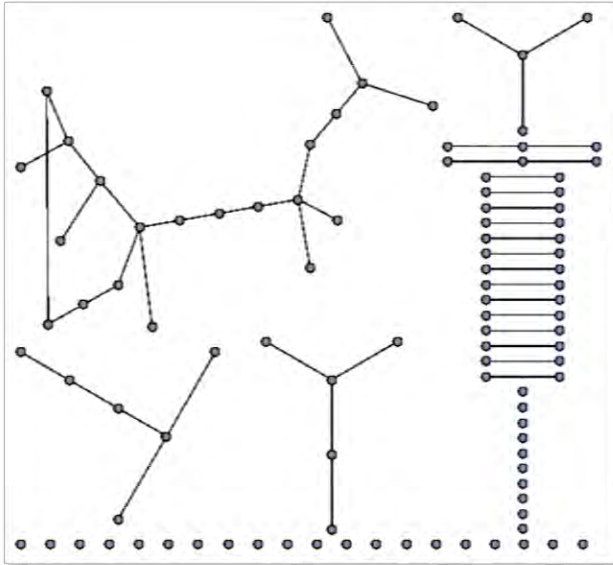
$$N \times N = 50 \times 50$$

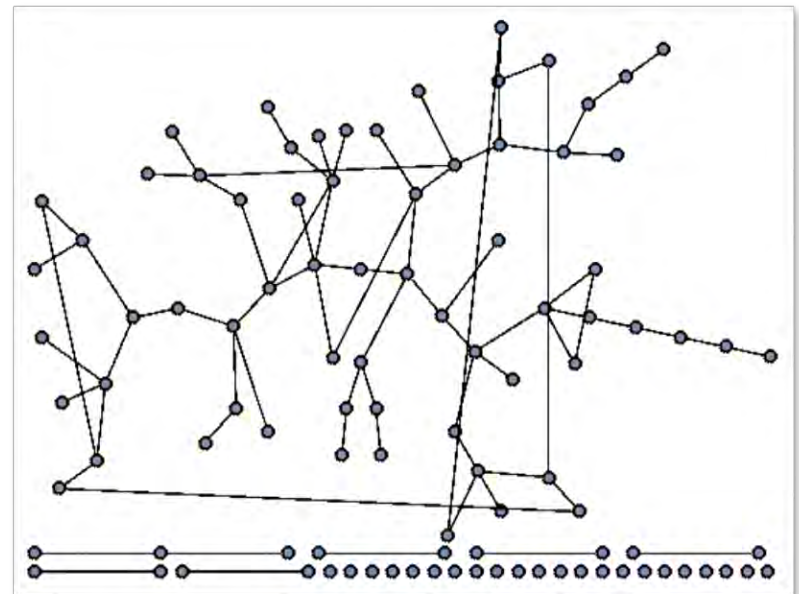
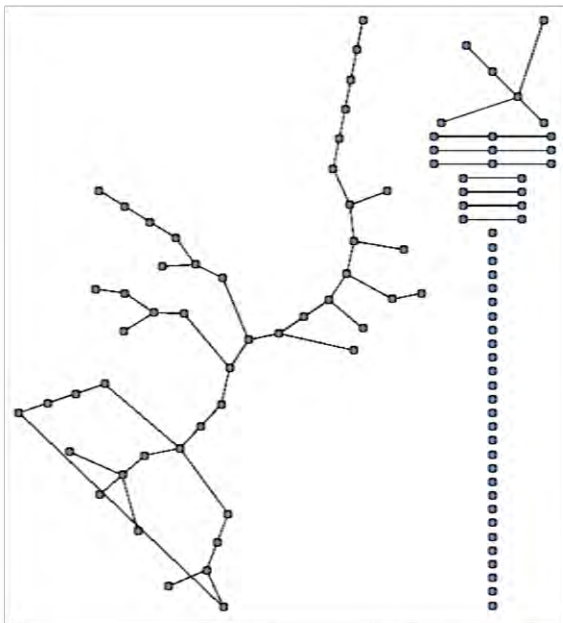
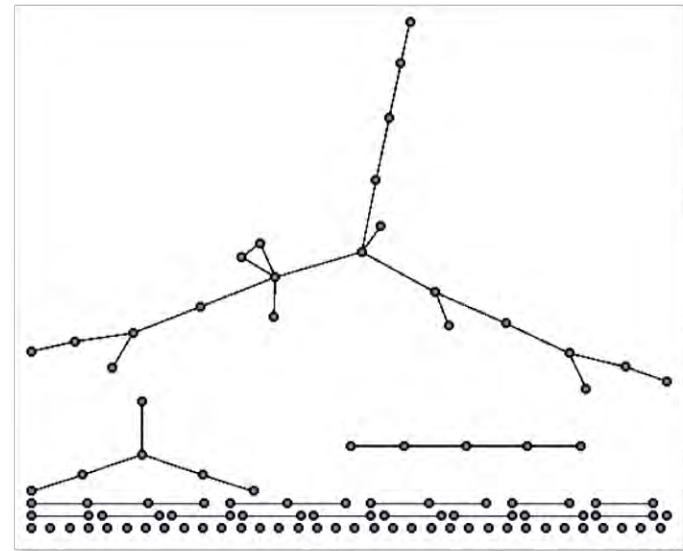
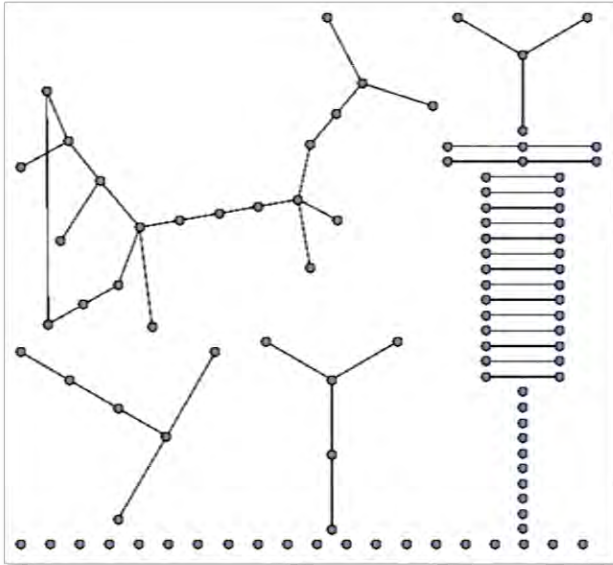


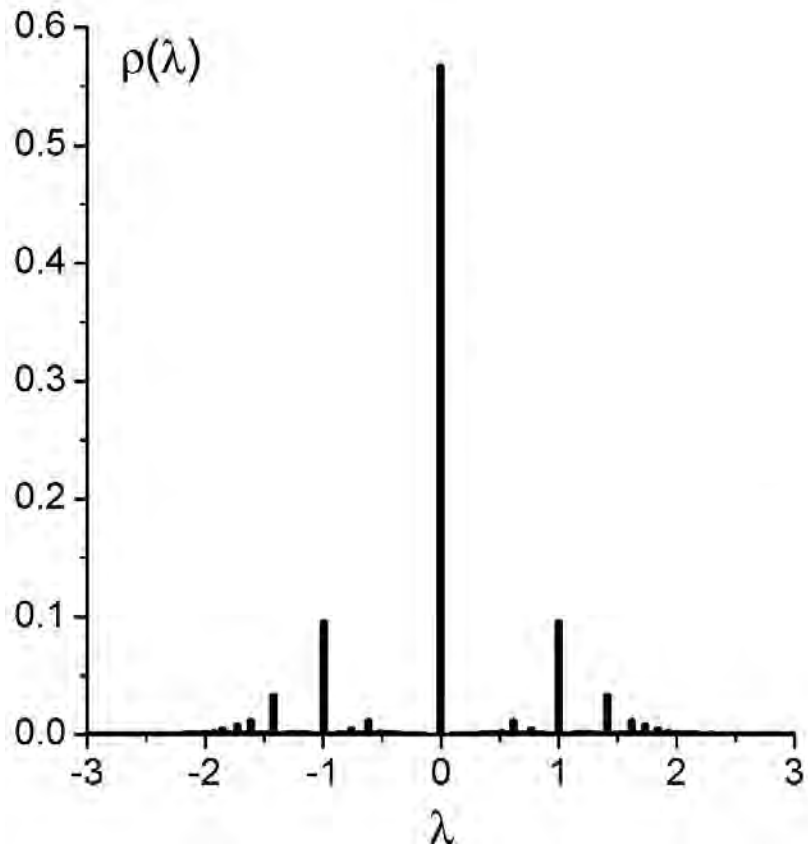
$r = \frac{1}{N}$, corresponds to percolation ($N \gg 1$)



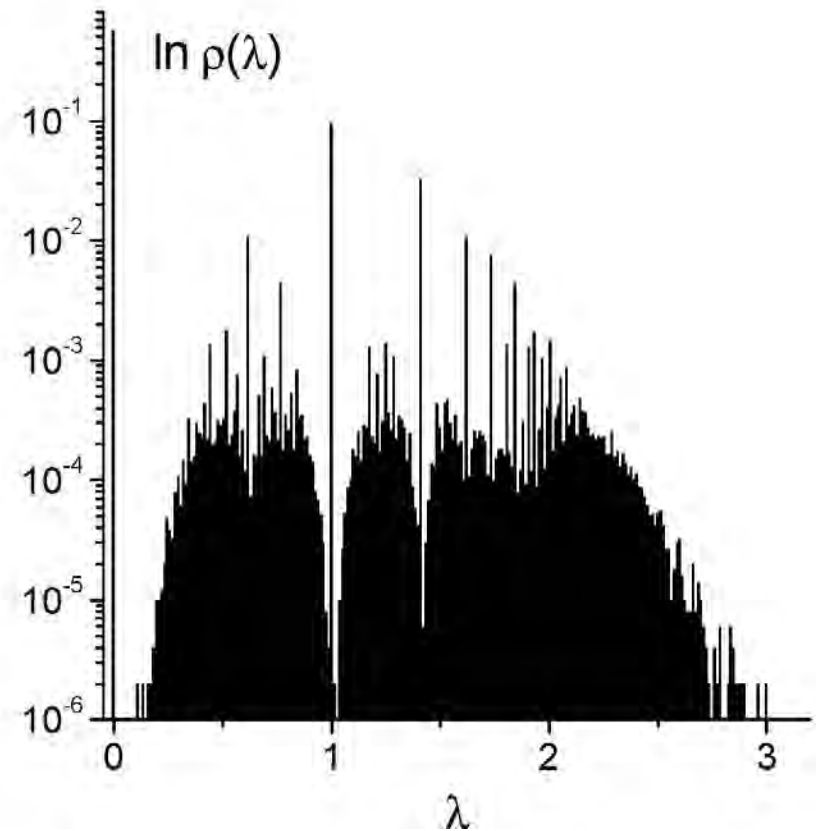
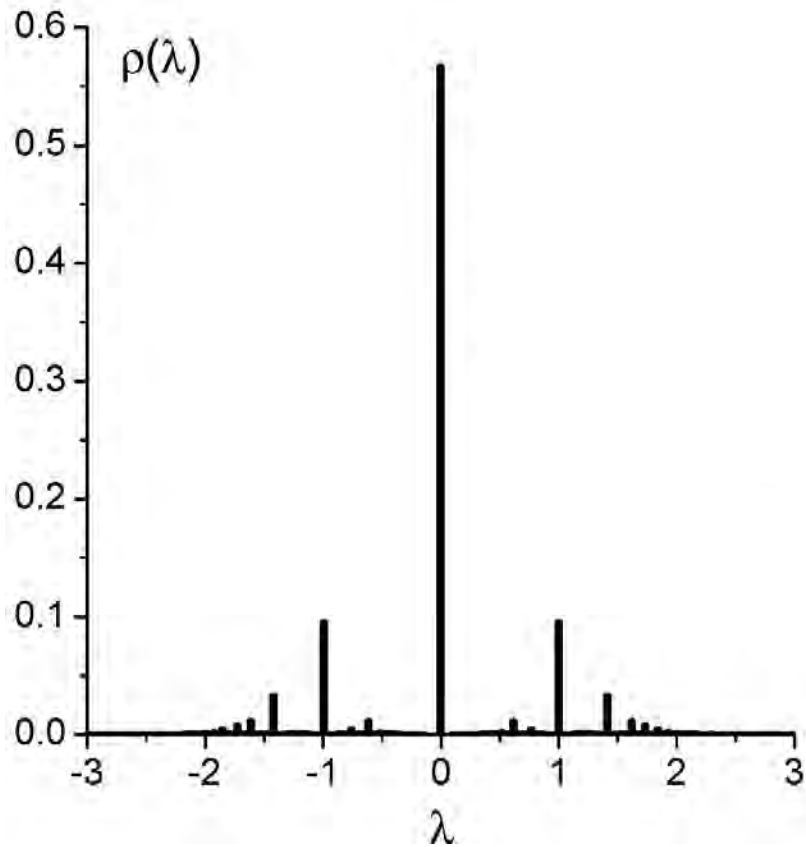








Spectral density $\rho(\lambda)$ of sparse random graphs at percolation point

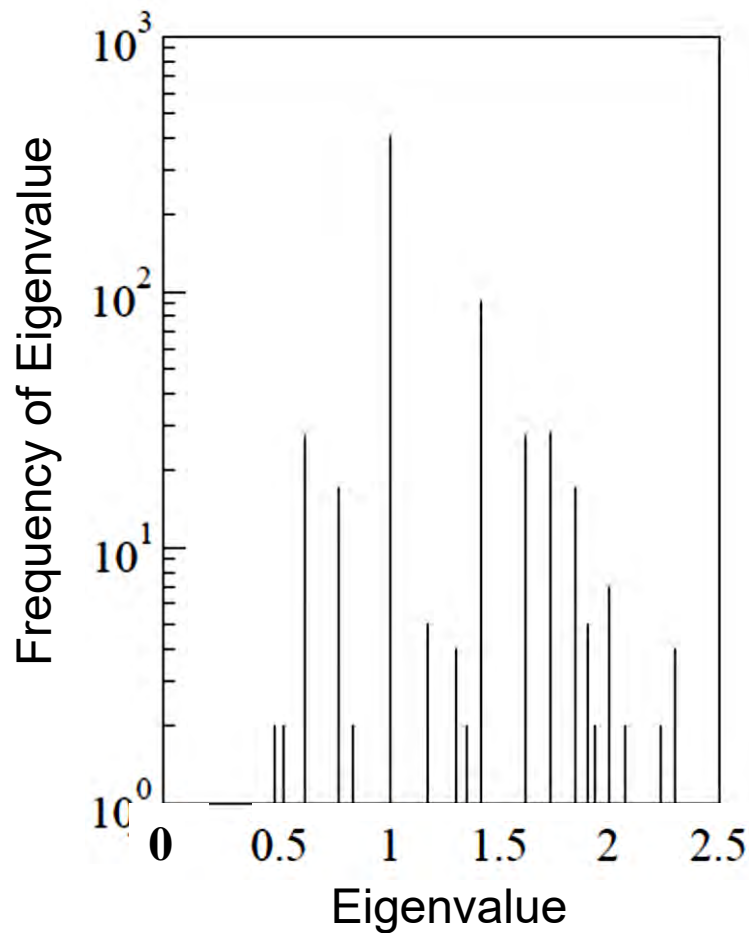


Semi-logarithmic plot for $\lambda > 0$

Spectral density $\rho(\lambda)$ of sparse random graphs at percolation point

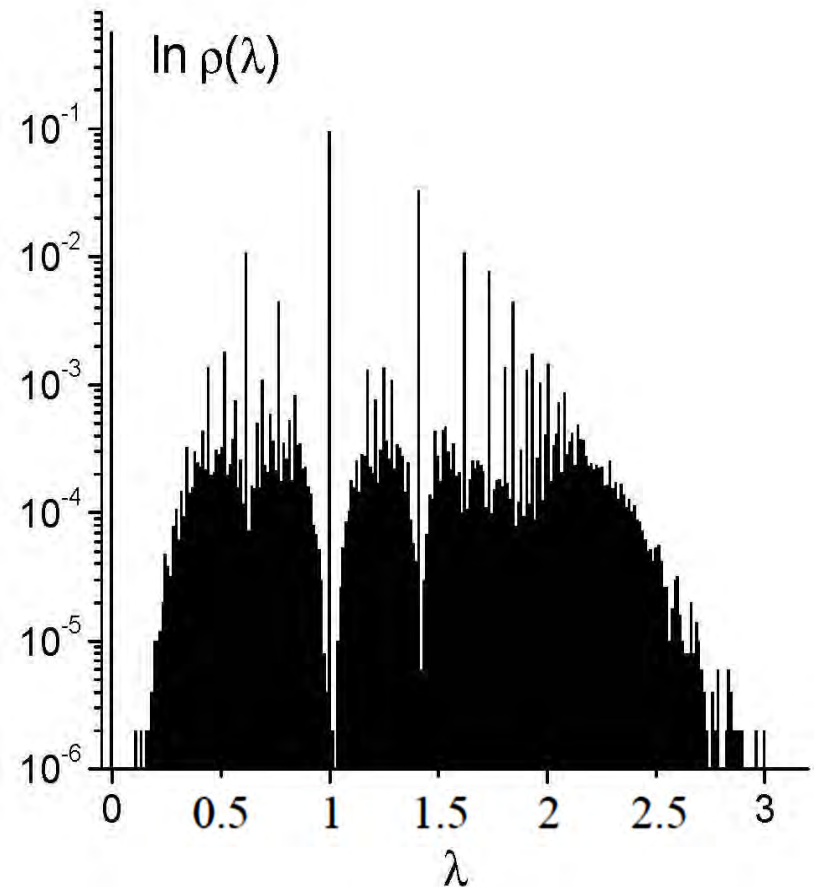
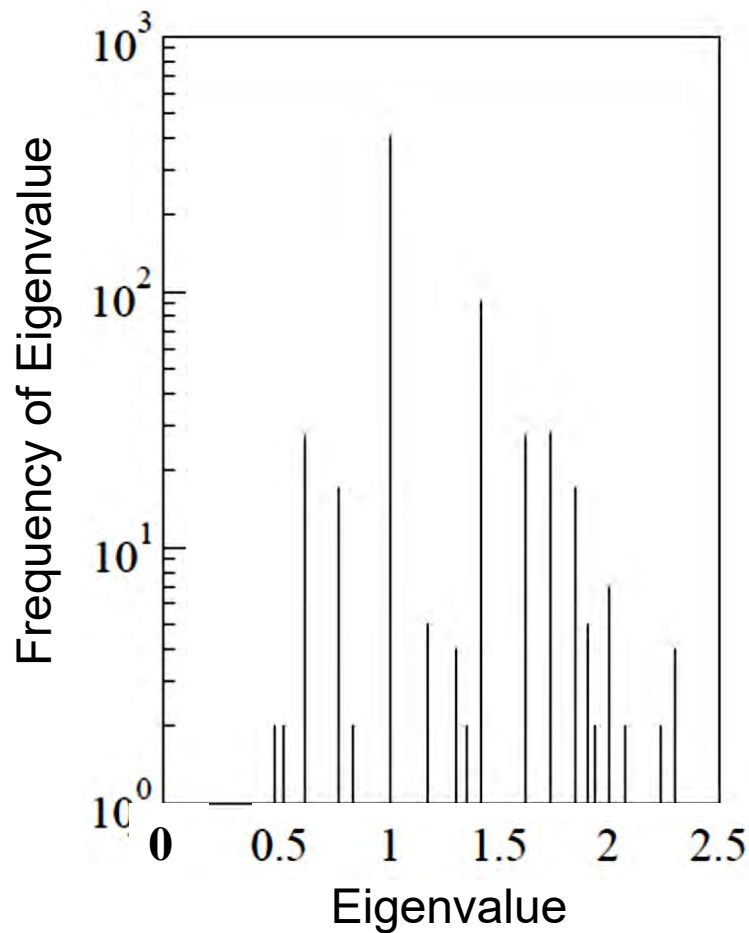
Spectral statistics of protein-protein interaction network in *Drosophyla melanogaster*

C. Kamp, K. Christensen, Phys. Rev. E (2005)

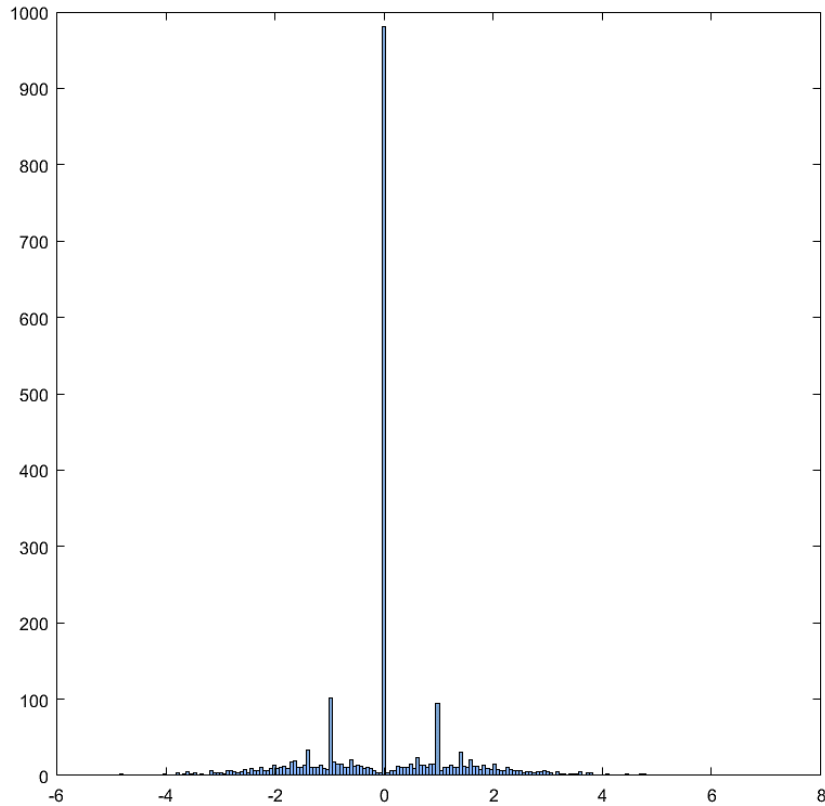


Spectral statistics of protein-protein interaction network in *Drosophyla melanogaster*

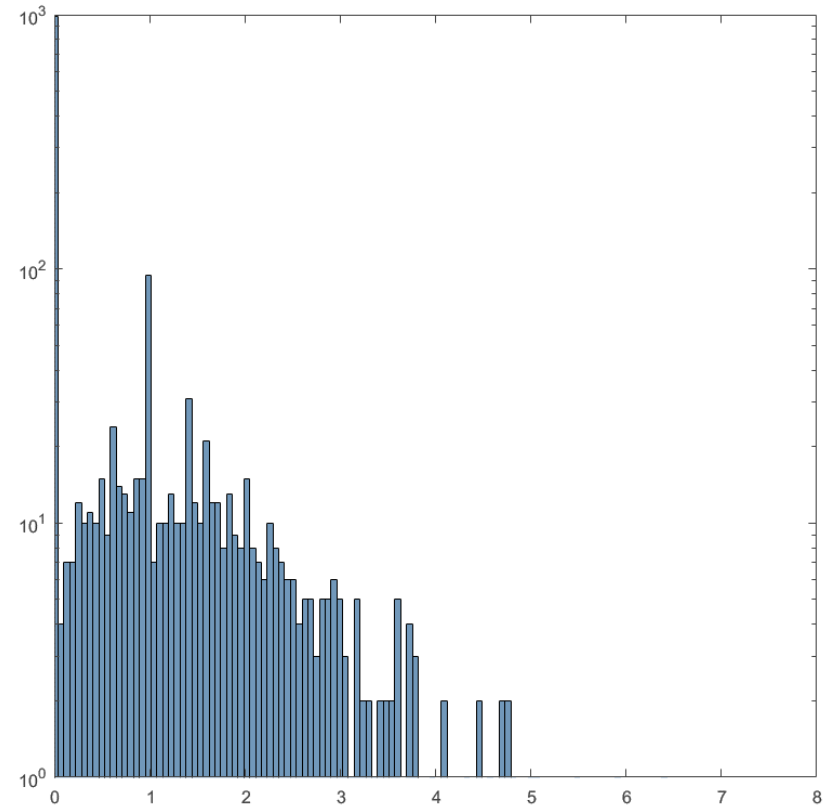
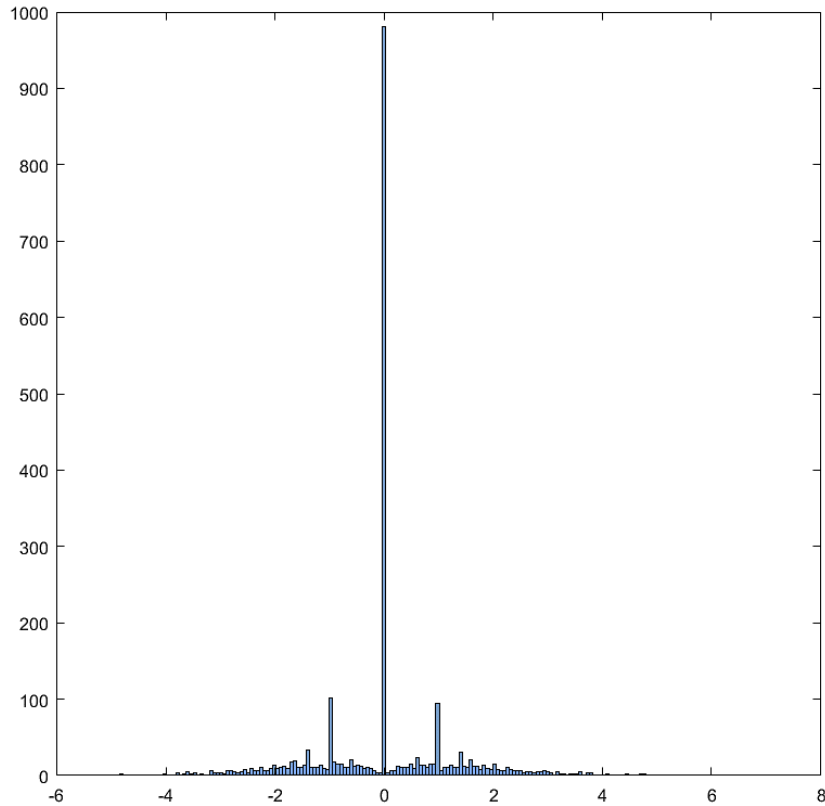
C. Kamp, K. Christensen, Phys. Rev. E (2005)



Sample of spectral statistics of adjacency matrix of X chromosome in single-cell experiments (resolution 10 kb)

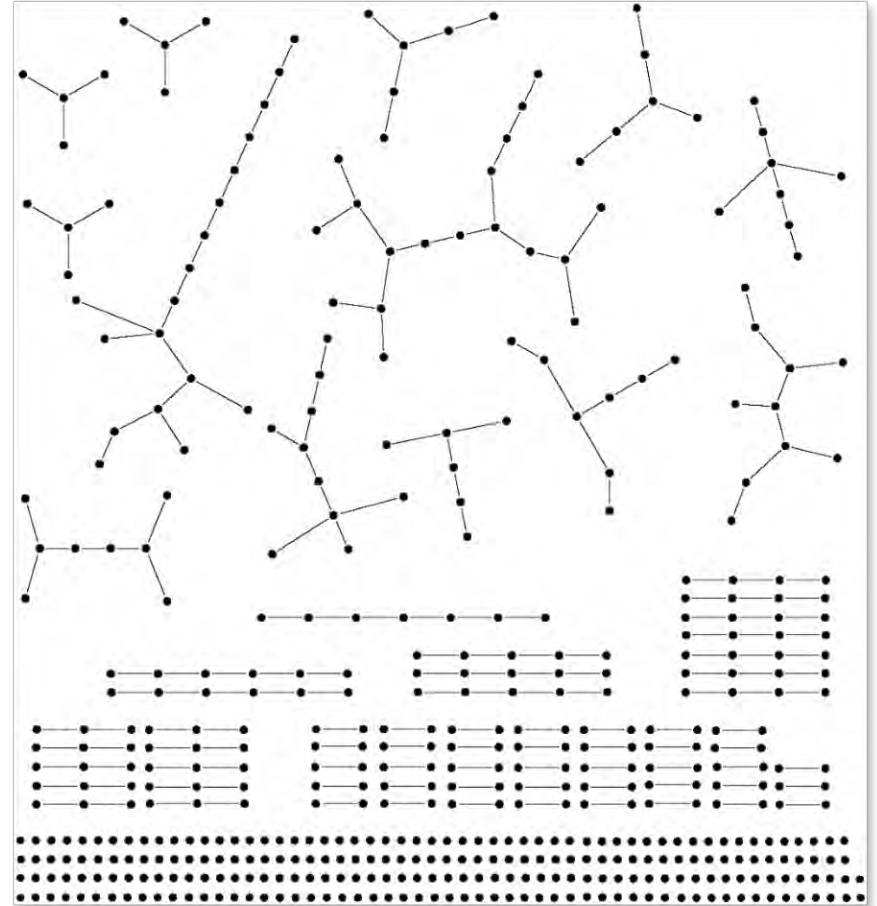
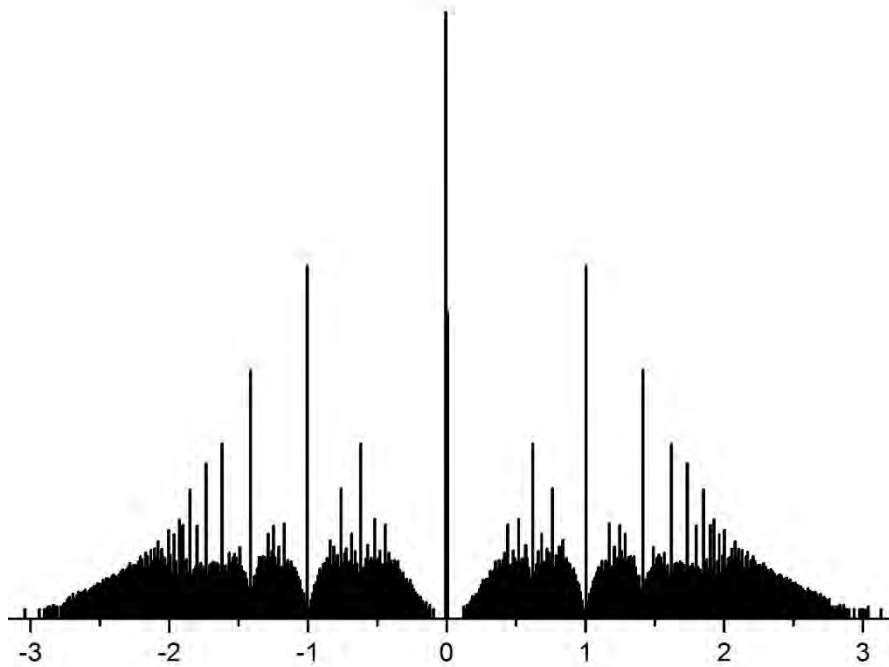


Sample of spectral statistics of adjacency matrix of X chromosome in single-cell experiments (resolution 10 kb)

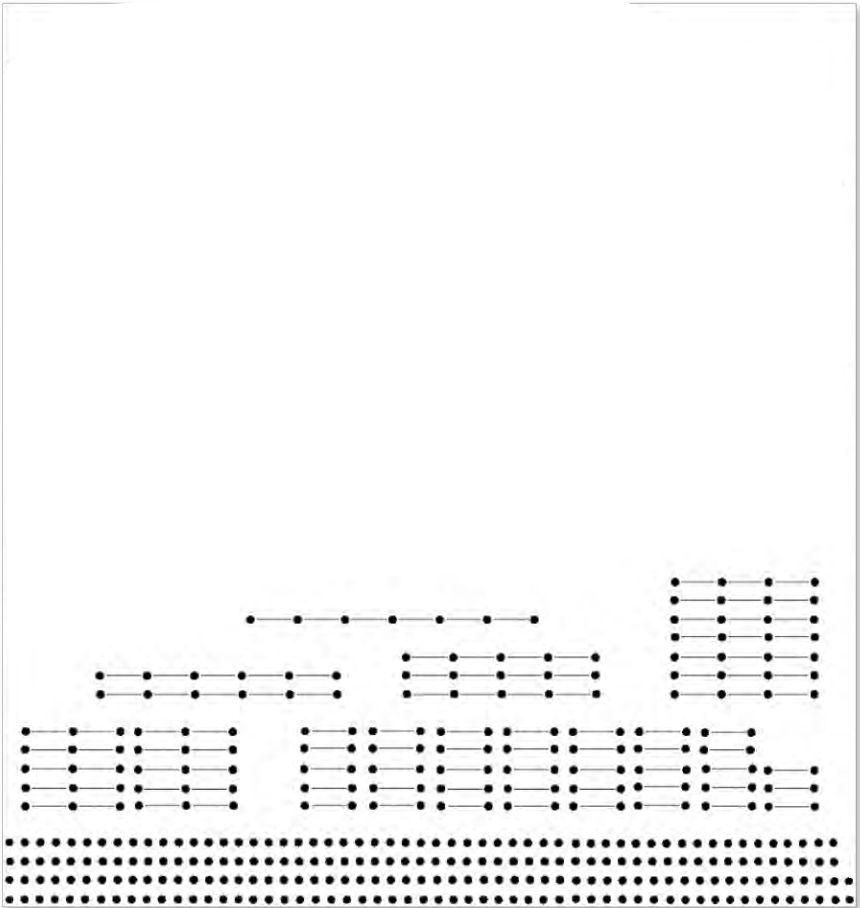
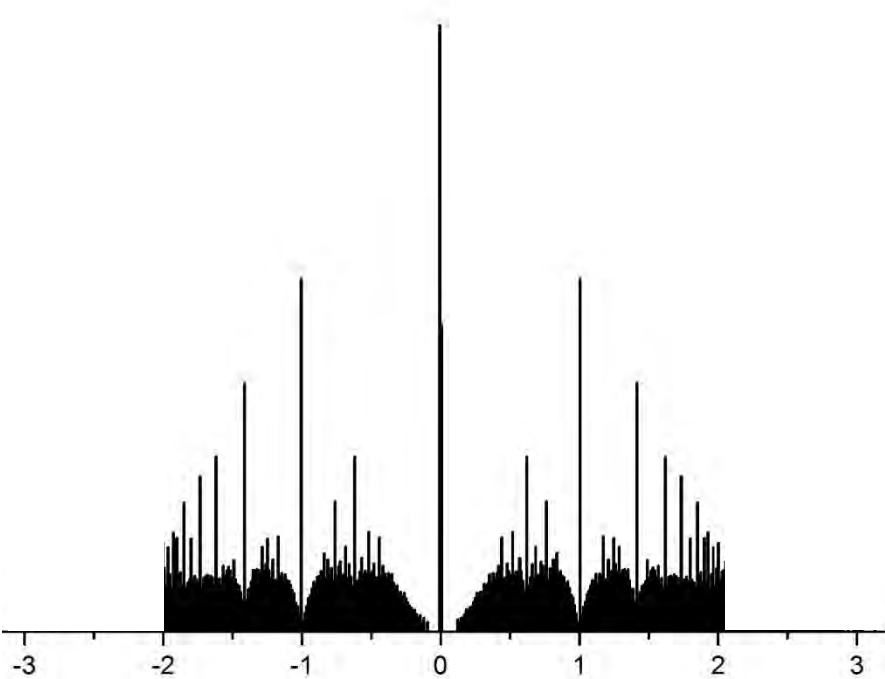


Semi-logarithmic plot

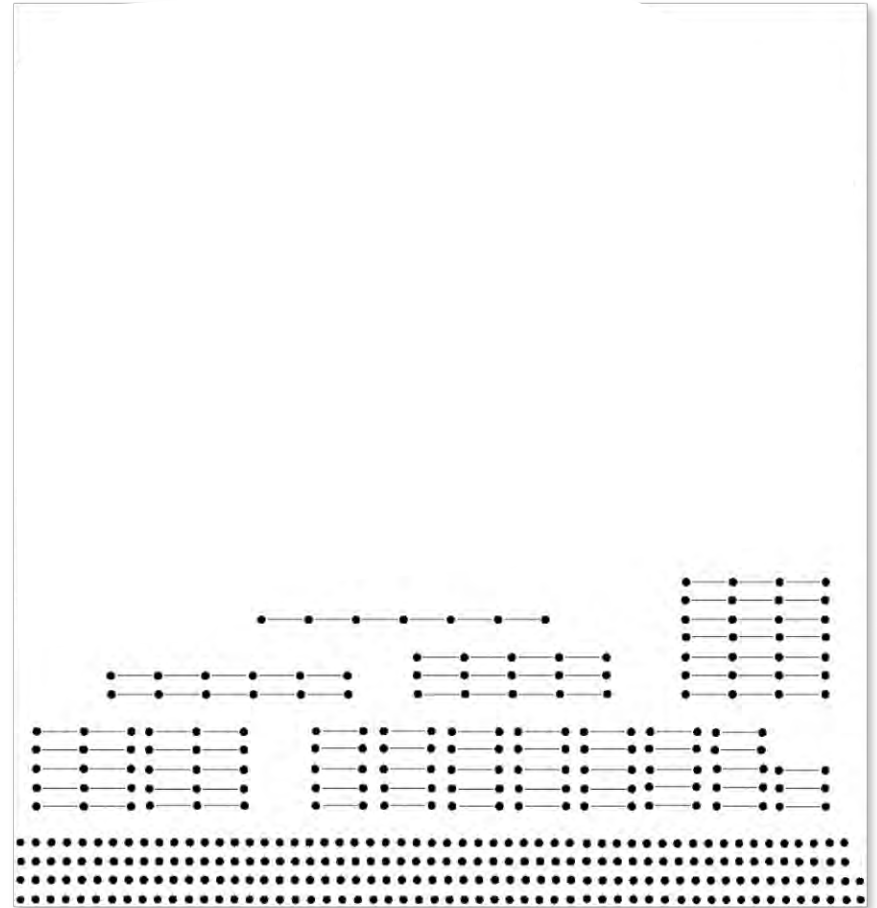
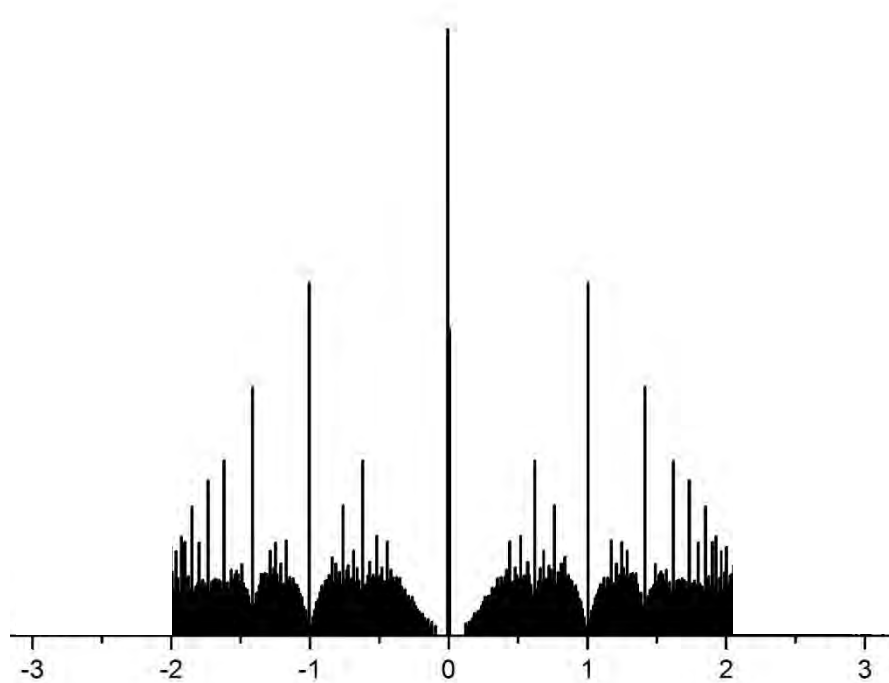
We have computed the distribution of **all** clusters in sizes, and separately – of clusters of **linear chains** only



We have computed the distribution of **all** clusters in sizes, and separately – of clusters of **linear chains** only



We have computed the distribution of **all** clusters in sizes, and separately – of clusters of **linear chains** only



$\left(\frac{2 - e^{-1}}{e - 1} \right) \times 100\% \approx 95\%$ of all random subgraphs at percolation are linear “polymers” with distribution $P(n) \sim e^{-n}$

Consider an ensemble of two(three)-diagonal matrices

$$\begin{pmatrix} 0 & x_1 & 0 & 0 & \dots \\ x_1 & 0 & x_2 & 0 & \\ 0 & x_2 & 0 & x_3 & \\ 0 & 0 & x_3 & 0 & \\ \vdots & & & & \ddots \end{pmatrix}$$

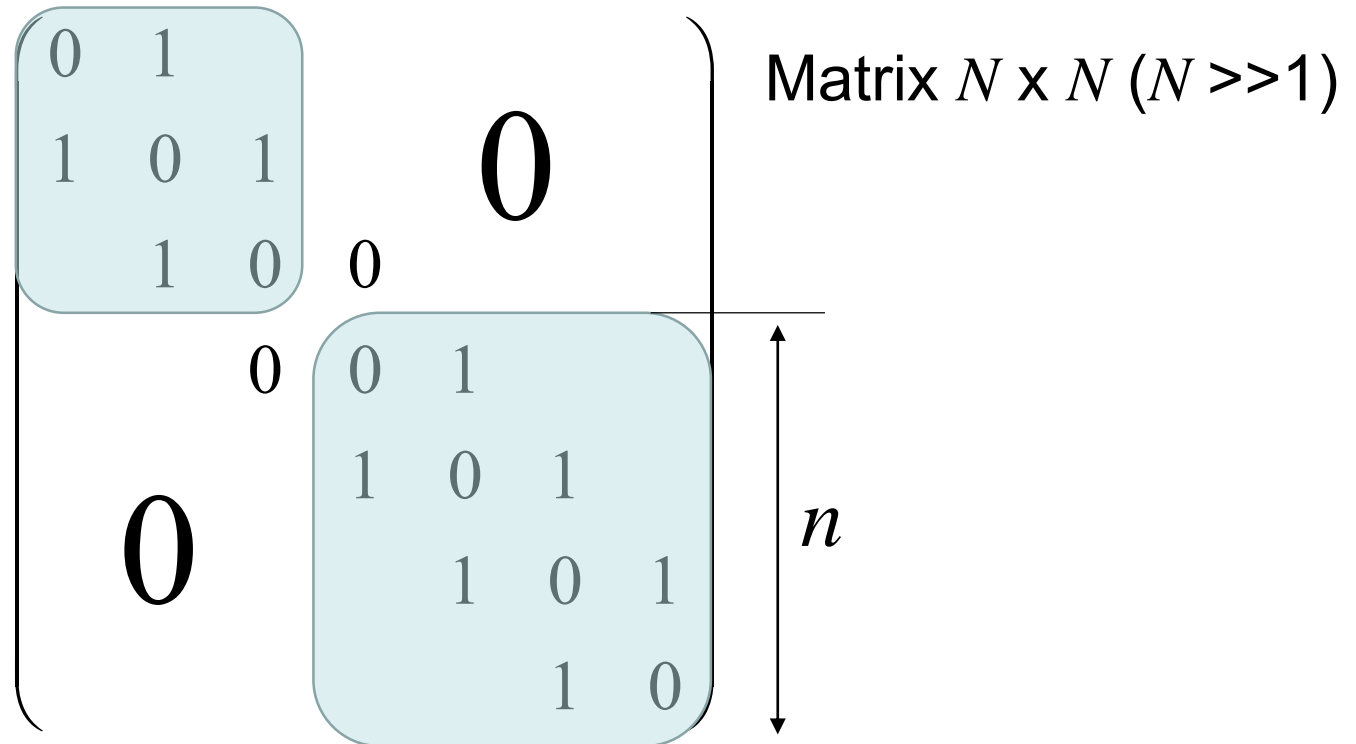
where the matrix elements are

$$x_i = \begin{cases} 1 & \text{with probability } q \\ 0 & \text{with probability } 1 - q \end{cases}$$

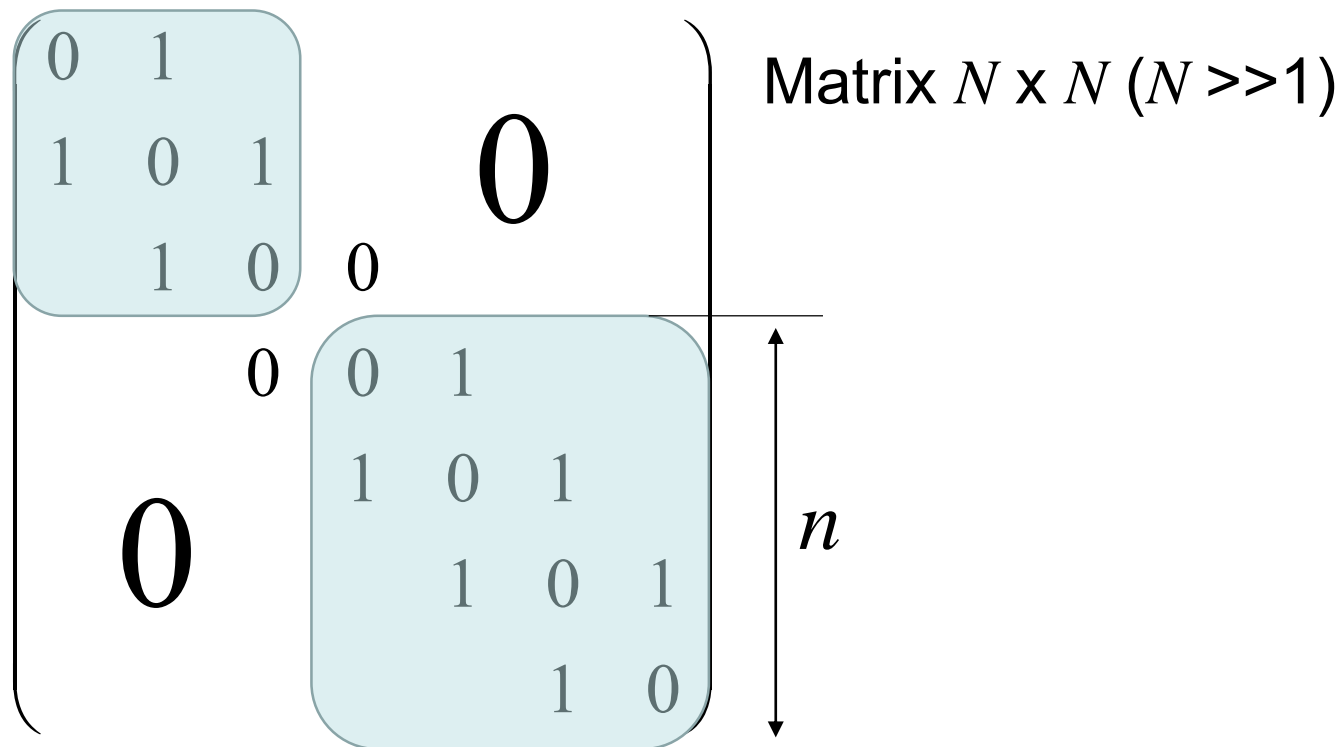
$$\begin{pmatrix} 0 & 1 & & & & & \\ 1 & 0 & 1 & & & & \\ & 1 & 0 & 0 & & & \\ & & 0 & 0 & 1 & & \\ & & & 1 & 0 & 1 & \\ \mathbf{0} & & & & 1 & 0 & 1 \\ & & & & & 1 & 0 \end{pmatrix}$$

Matrix $N \times N$ ($N \gg 1$)

Adjacency matrix splits in uniform Jordan cells with the distribution $\sim q^n$ ($0 < q < 1$) in sizes



Adjacency matrix splits in uniform Jordan cells with the distribution $\sim q^n$ ($0 < q < 1$) in sizes



The set of eigenvalues in the cell of size $n \times n$ is

$$\lambda_k = 2 \cos \frac{\pi k}{n+1}; \quad (k = 1, \dots, n)$$

Spectral density, $\rho_{\text{lin}}(\lambda)$, of the ensemble of random matrices is:

$$\rho_{\text{lin}}(\lambda) = \lim_{N \rightarrow \infty} \frac{1}{N} \left\langle \sum_{k=1}^N \delta(\lambda - \lambda_k) \right\rangle$$

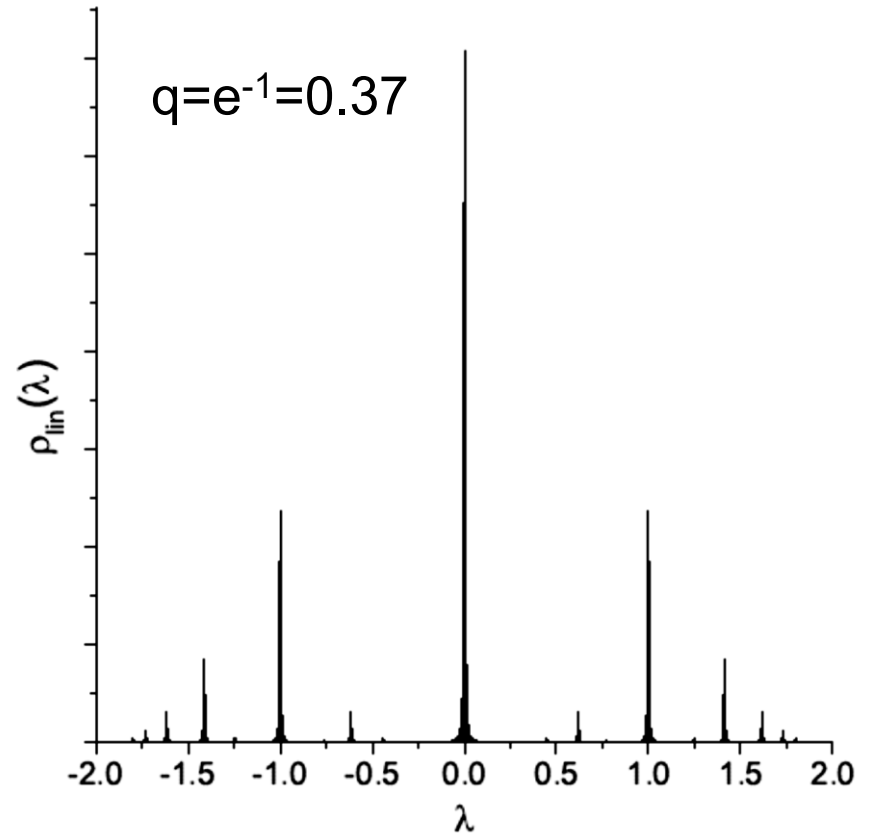
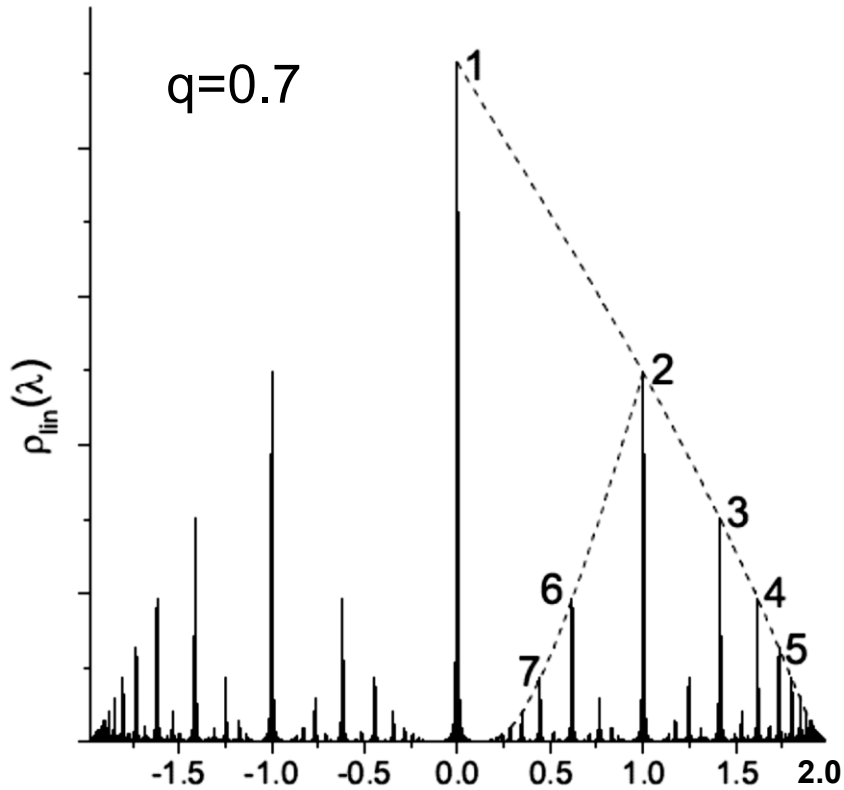
Spectral density, $\rho_{\text{lin}}(\lambda)$, of the ensemble of random matrices is:

$$\rho_{\text{lin}}(\lambda) = \lim_{N \rightarrow \infty} \frac{1}{N} \left\langle \sum_{k=1}^N \delta(\lambda - \lambda_k) \right\rangle$$

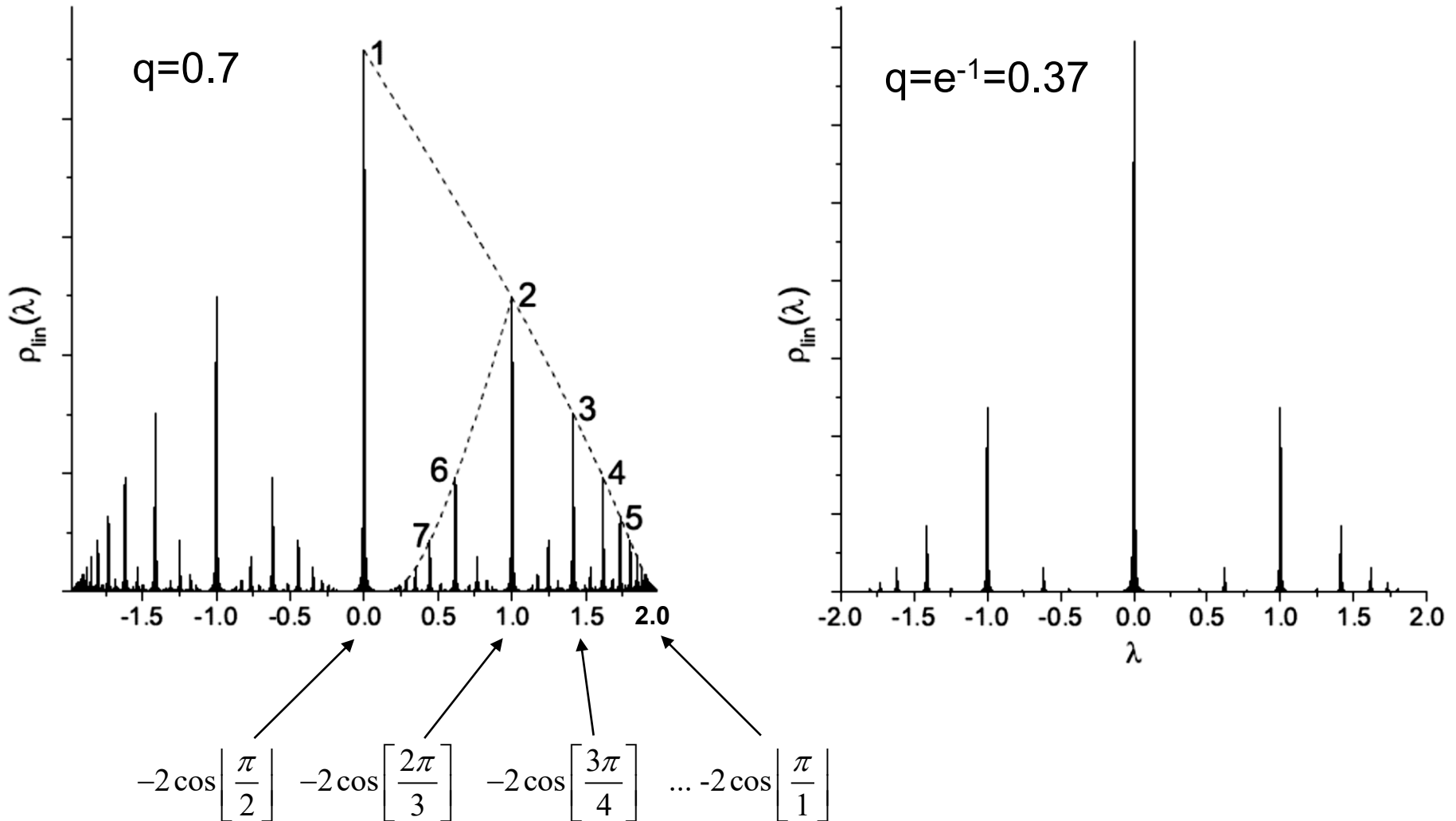
Summing the spectra of exponentially weighted Jordan cells, we get:

$$\rho_{\text{lin}}(\lambda) = \lim_{\substack{N \rightarrow \infty \\ \varepsilon \rightarrow 0}} \frac{\varepsilon}{\pi N} \sum_{n=1}^N q^n \sum_{k=1}^n \frac{1}{(\lambda - 2 \cos \frac{\pi k}{n+1})^2 + \varepsilon^2}$$

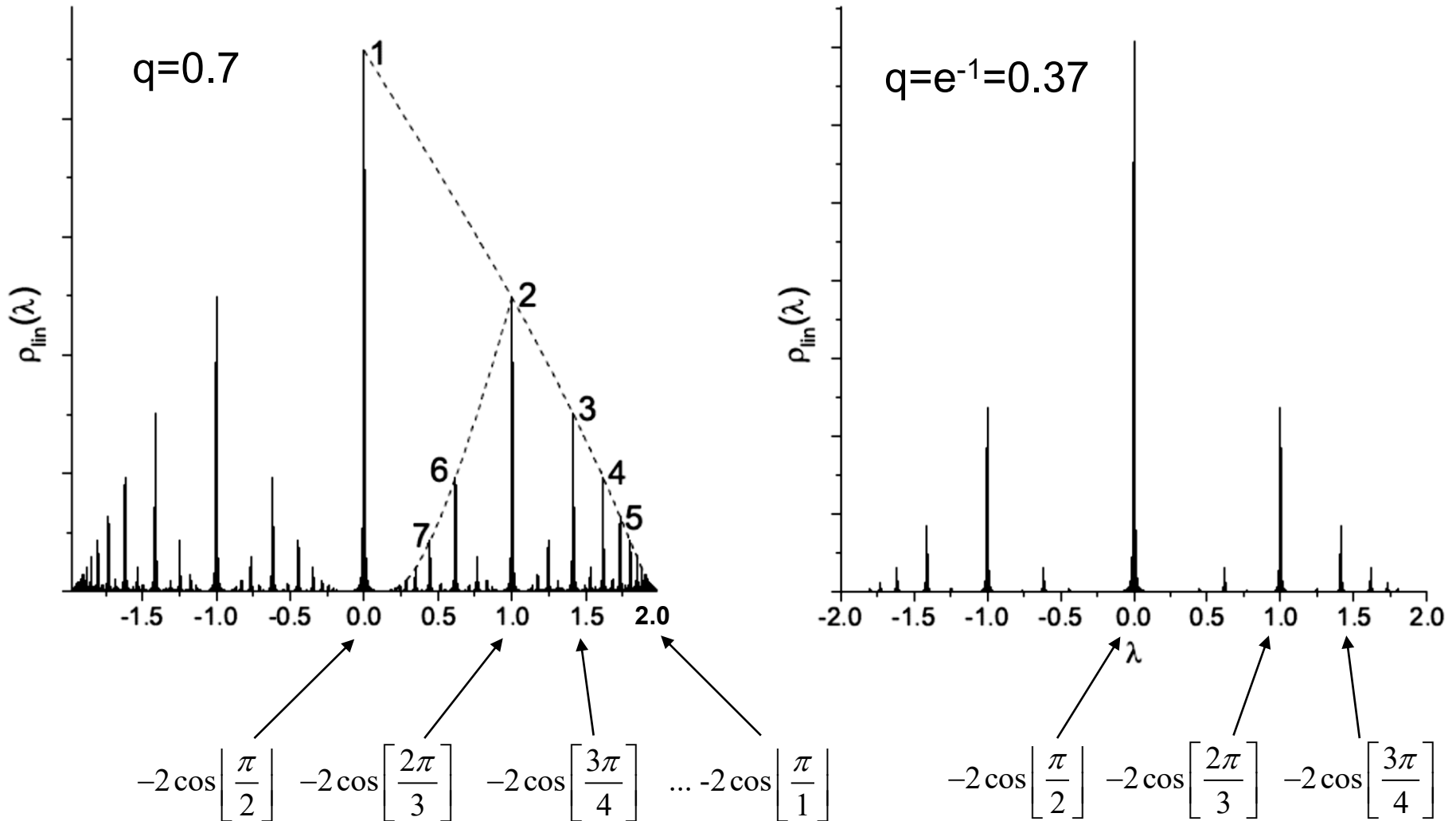
Spectral density of an ensemble of random three-diagonal operators



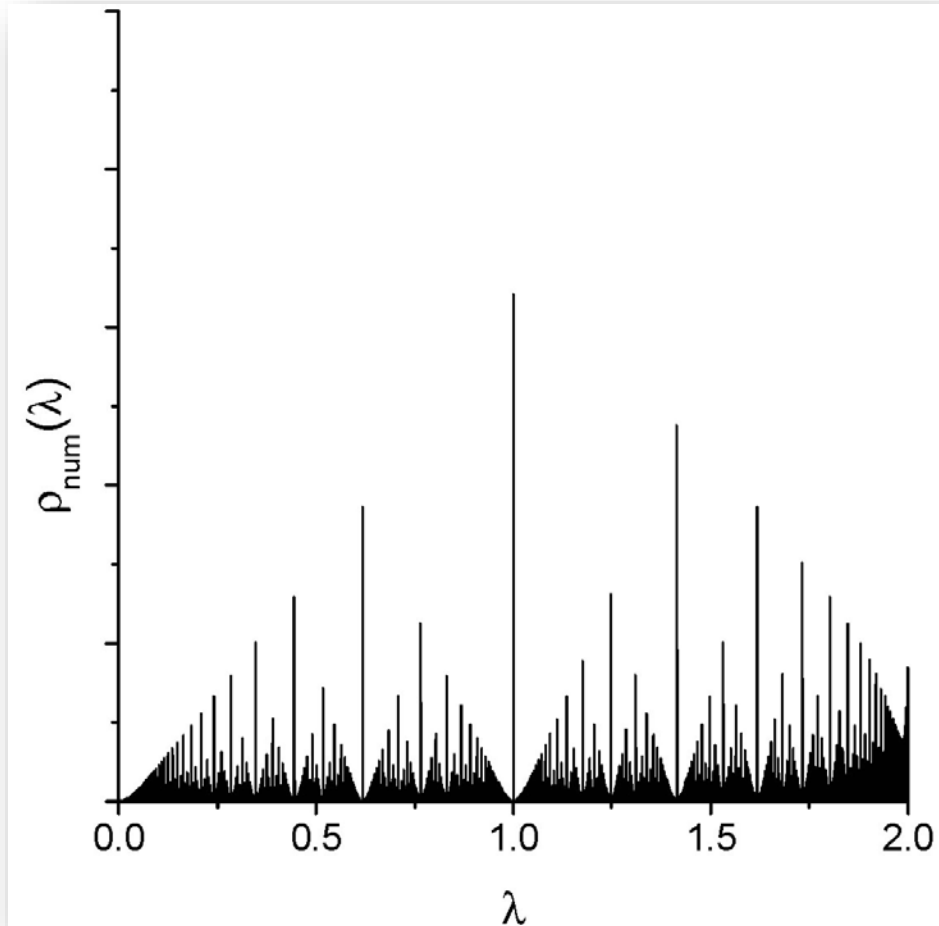
Spectral density of an ensemble of random three-diagonal operators



Spectral density of an ensemble of random three-diagonal operators



Could we get analytic expression for a limiting form (at $q \rightarrow 1$) of the full spectral density, $\rho_{\text{lin}}(\lambda)$?



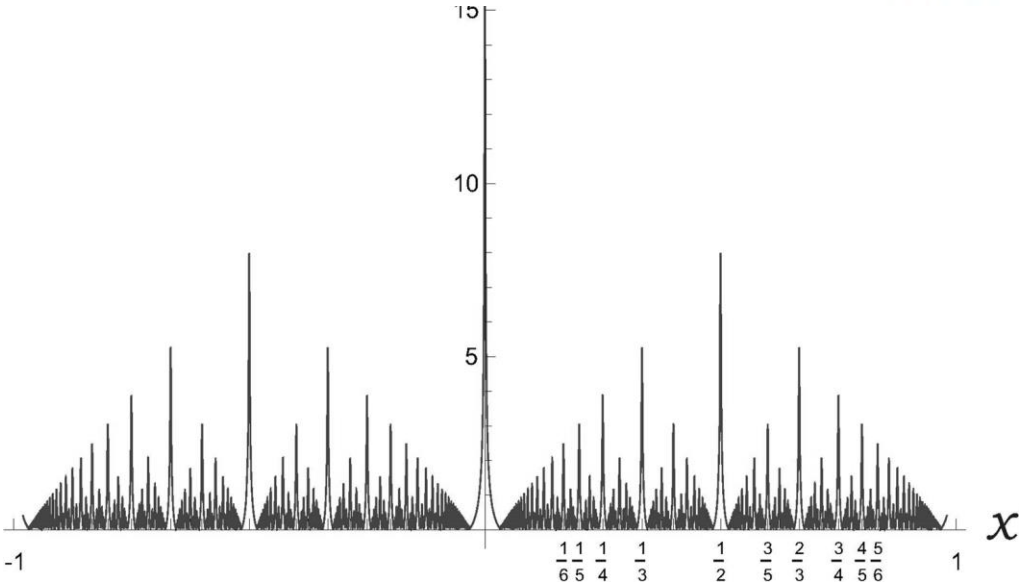
Some plots on the basis of Dedekind η – function

$$\eta(z) = e^{\pi iz/12} \prod_{n=0}^{\infty} (1 - e^{2\pi inz}); \quad z = x + iy \quad (y > 0)$$

Some plots on the basis of Dedekind η – function

$$\eta(z) = e^{\pi iz/12} \prod_{n=0}^{\infty} (1 - e^{2\pi inz}); \quad z = x + iy \quad (y > 0)$$

$$\sqrt{-\ln \left| \eta(x + iy) \right|} \Big|_{y \rightarrow 0+}$$

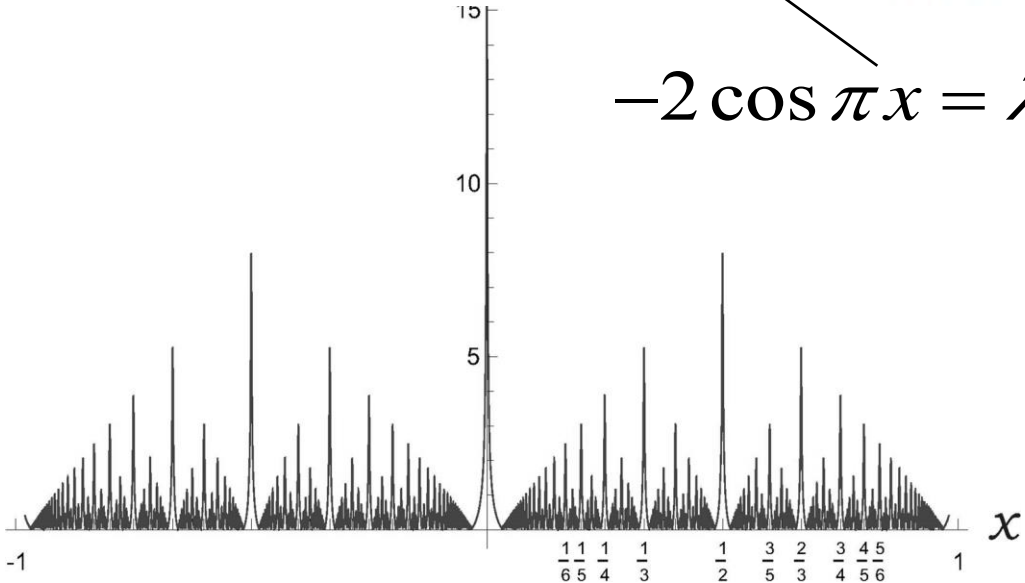


Some plots on the basis of Dedekind η – function

$$\eta(z) = e^{\pi iz/12} \prod_{n=0}^{\infty} (1 - e^{2\pi inz}); \quad z = x + iy \quad (y > 0)$$

$$\sqrt{-\ln \left| \eta \left(x + iy \right) \right|} \Big|_{y \rightarrow 0+}$$

$$-2 \cos \pi x = \lambda$$



Spectral density $\rho_{\text{lin}}(\lambda)$ of ensemble of exponentially weighted random 3-diagonal matrices at $q \rightarrow 1$

$$\rho_{\text{lin}}(\lambda) = \lim_{\substack{N \rightarrow \infty \\ \varepsilon \rightarrow 0}} \frac{\varepsilon}{\pi N} \sum_{n=1}^N q^n \sum_{k=1}^n \frac{1}{\left(\lambda - 2 \cos \frac{\pi k}{n+1}\right)^2 + \varepsilon^2}$$

Spectral density $\rho_{\text{lin}}(\lambda)$ of ensemble of exponentially weighted random 3-diagonal matrices at $q \rightarrow 1$

$$\rho_{\text{lin}}(\lambda) = \lim_{\substack{N \rightarrow \infty \\ \varepsilon \rightarrow 0}} \frac{\varepsilon}{\pi N} \sum_{n=1}^N q^n \sum_{k=1}^n \frac{1}{\left(\lambda - 2 \cos \frac{\pi k}{n+1}\right)^2 + \varepsilon^2}$$

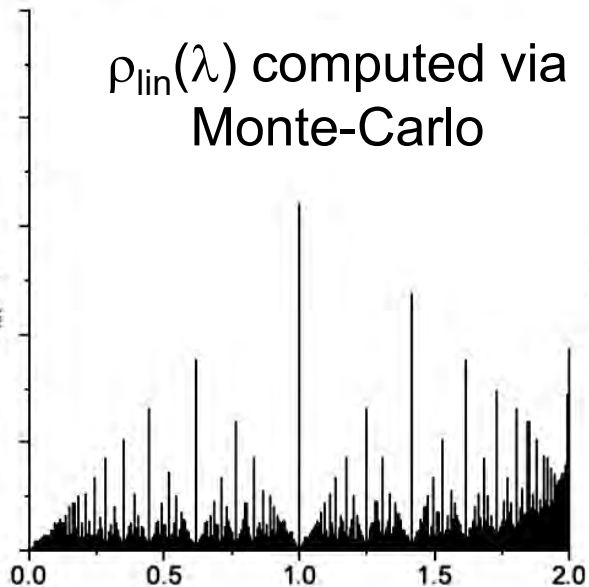
$$\lim_{q \rightarrow 1^-} \frac{\rho_{\text{lin}}(\lambda, q)}{\sqrt{-\ln \left| \eta \left(\frac{1}{\pi} \arccos(-\lambda/2) + i \frac{(1-q)^2}{12\pi} \right) \right|}} = 1$$

Spectral density $\rho_{\text{lin}}(\lambda)$ of ensemble of exponentially weighted random 3-diagonal matrices at $q \rightarrow 1$

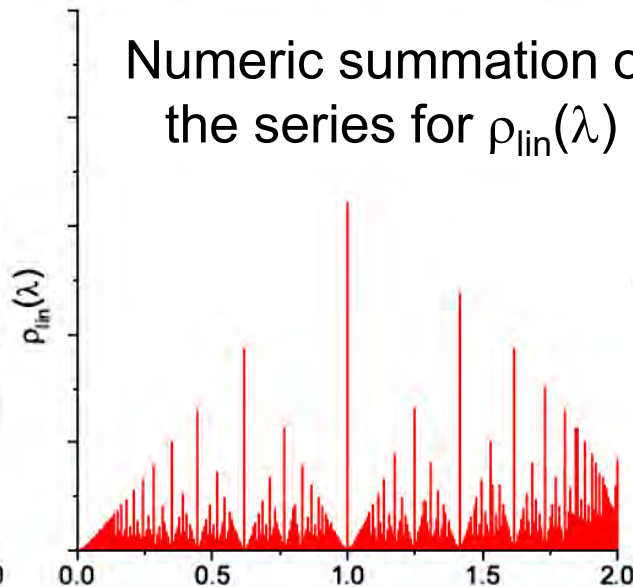
$$\rho_{\text{lin}}(\lambda) = \lim_{\substack{N \rightarrow \infty \\ \varepsilon \rightarrow 0}} \frac{\varepsilon}{\pi N} \sum_{n=1}^N q^n \sum_{k=1}^n \frac{1}{\left(\lambda - 2 \cos \frac{\pi k}{n+1}\right)^2 + \varepsilon^2}$$

$$\lim_{q \rightarrow 1^-} \frac{\rho_{\text{lin}}(\lambda, q)}{\sqrt{-\ln \left| \eta \left(\frac{1}{\pi} \arccos(-\lambda/2) + i \frac{(1-q)^2}{12\pi} \right) \right|}} = 1$$

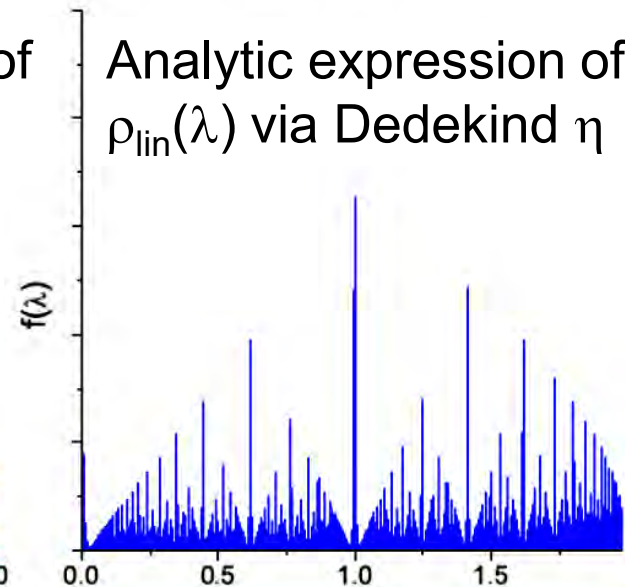
$\rho_{\text{lin}}(\lambda)$ computed via Monte-Carlo



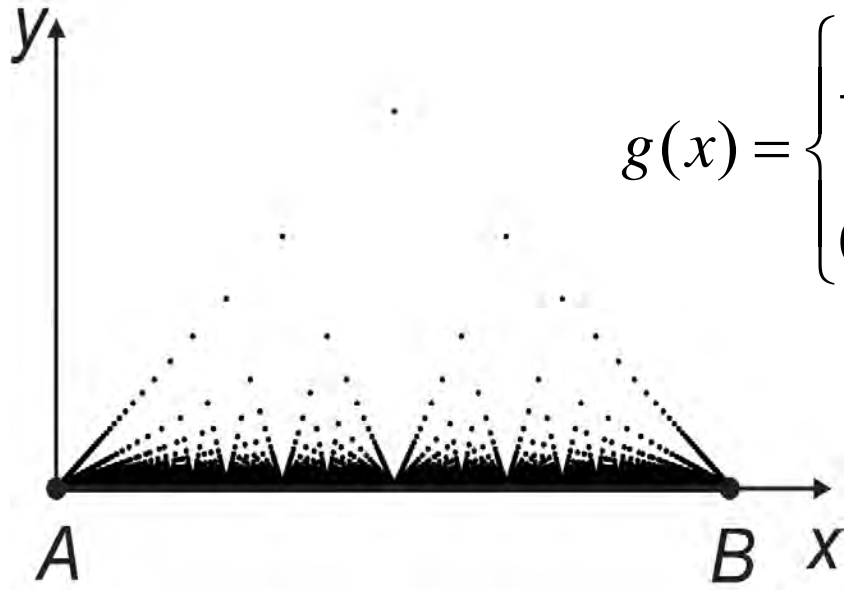
Numeric summation of the series for $\rho_{\text{lin}}(\lambda)$



Analytic expression of $\rho_{\text{lin}}(\lambda)$ via Dedekind η

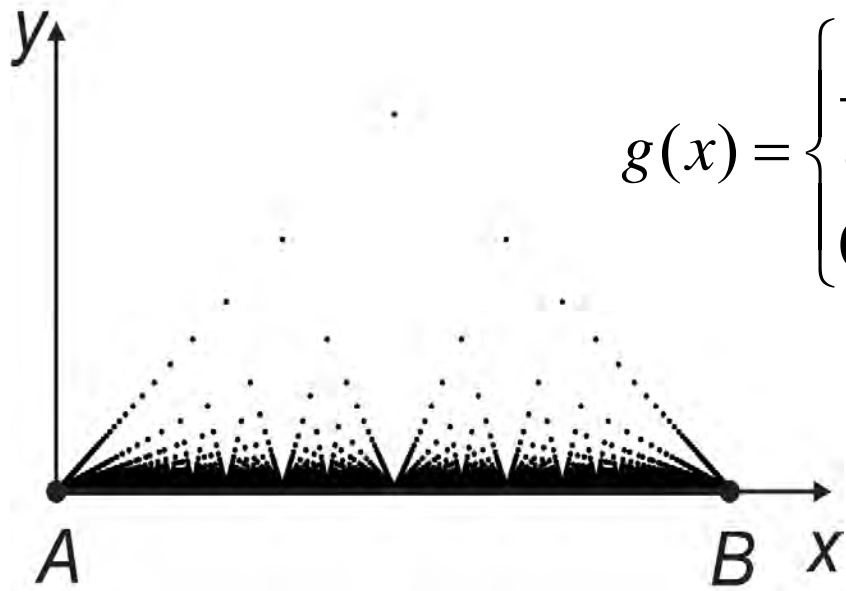


Thomae function, Dedekind η and Euclid orchard

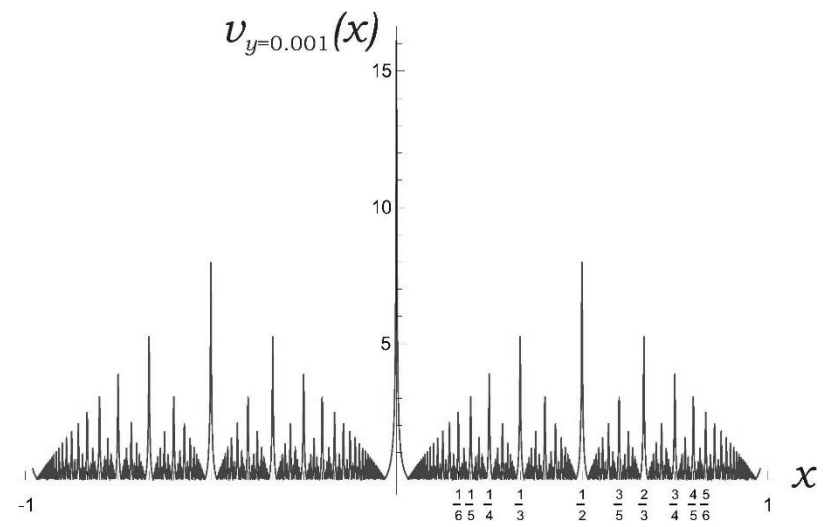


$$g(x) = \begin{cases} \frac{1}{q} & \text{if } x = \frac{p}{q} \text{ and } (p, q) \text{ are coprime} \\ 0 & x \text{ otherwise} \end{cases}$$

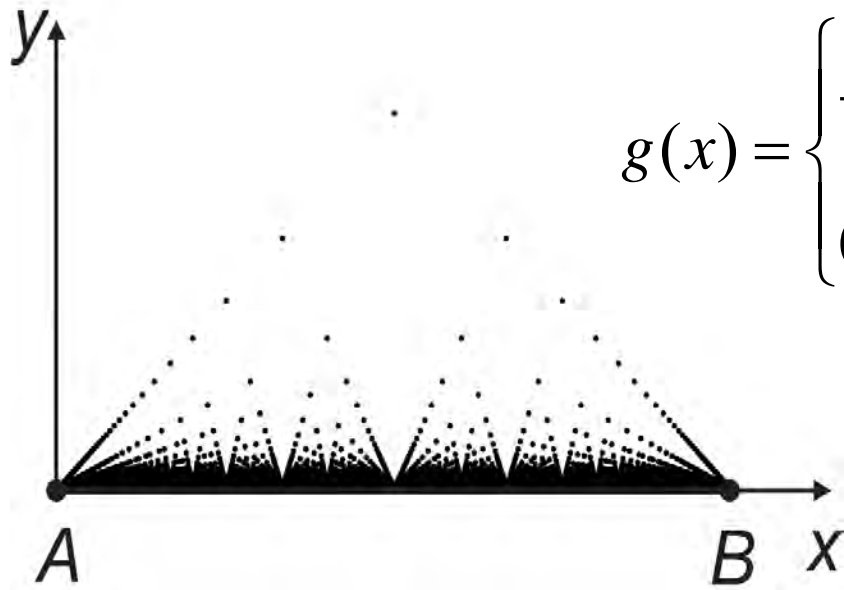
Thomae function, Dedekind η and Euclid orchard



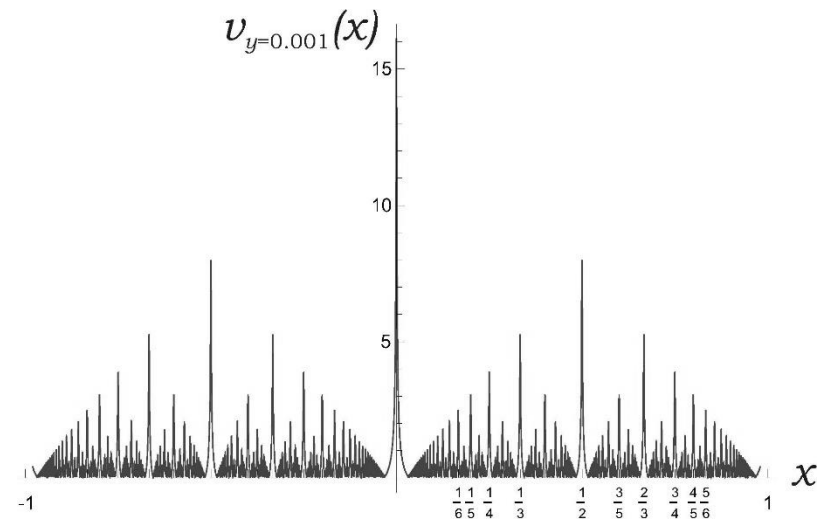
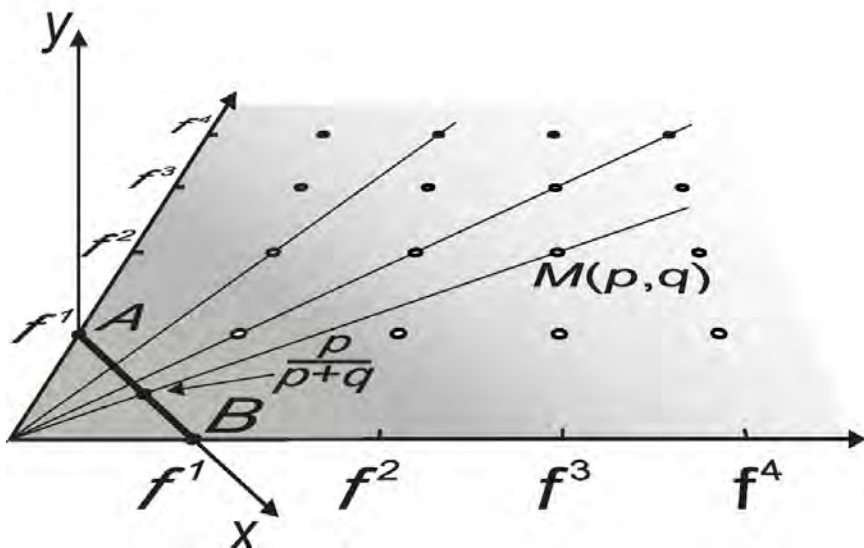
$$g(x) = \begin{cases} \frac{1}{q} & \text{if } x = \frac{p}{q} \text{ and } (p, q) \text{ are coprime} \\ 0 & x \text{ otherwise} \end{cases}$$



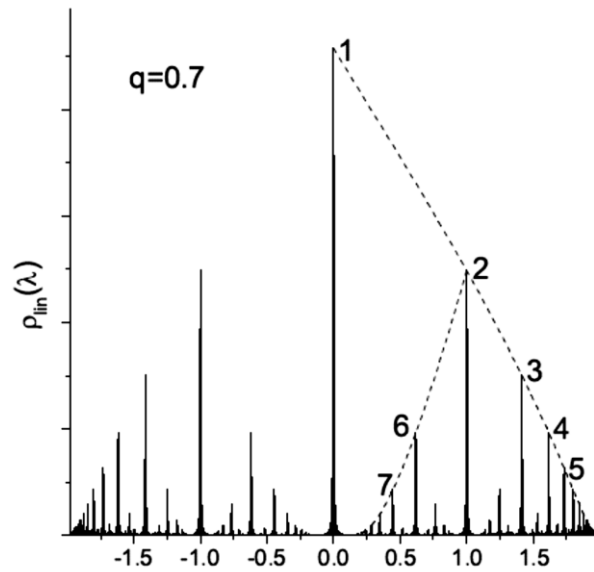
Thomae function, Dedekind η and Euclid orchard



$$g(x) = \begin{cases} \frac{1}{q} & \text{if } x = \frac{p}{q} \text{ and } (p, q) \text{ are coprime} \\ 0 & \text{otherwise} \end{cases}$$



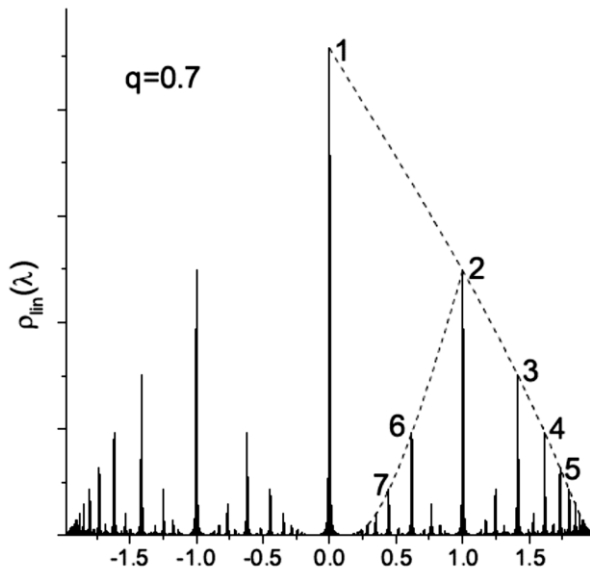
Spectrum tail for $q < 1$



$$S_1 : \lambda = -2 \cos \frac{\pi k}{k+1} \Big|_{k \rightarrow \infty} \rightarrow 2 - \frac{\pi^2}{k^2},$$

$$\rho^{S_1}(\lambda_k) \Big|_{k \rightarrow \infty} \rightarrow q^k$$

Spectrum tail for $q < 1$



$$S_1 : \lambda = -2 \cos \frac{\pi k}{k+1} \Big|_{k \rightarrow \infty} \rightarrow 2 - \frac{\pi^2}{k^2},$$

$$\rho^{S_1}(\lambda_k) \Big|_{k \rightarrow \infty} \rightarrow q^k$$

Lifshitz tail of 1D Anderson localization

$$\rho_{\text{lin}}^{S_1}(\lambda \rightarrow 2) \rightarrow q^{\pi/\sqrt{2-\lambda}} :$$

Laplace transform gives:

$$\rho(N) = \frac{1}{2\pi i} \oint \rho(\lambda) e^{N\lambda} d\lambda \Big|_{N \gg 1} \sim \varphi(N) e^{-aN - bN^{1/3}}$$

Modular Dedekind η – function is invariant
with respect to $SL(2, \mathbb{Z})$ group

$$\eta(z) = e^{\pi iz/12} \prod_{n=0}^{\infty} (1 - e^{2\pi inz}); \quad z = x + iy \quad (y > 0)$$

$$\eta(z + 1) = e^{\pi iz/12} \eta(z)$$

$$\eta\left(-\frac{1}{z}\right) = \sqrt{-i} \eta(z)$$

Modular Dedekind η – function is invariant
with respect to $SL(2, \mathbb{Z})$ group

$$\eta(z) = e^{\pi iz/12} \prod_{n=0}^{\infty} (1 - e^{2\pi inz}); \quad z = x + iy \quad (y > 0)$$

$$\eta(z + 1) = e^{\pi iz/12} \eta(z)$$

$$\eta\left(-\frac{1}{z}\right) = \sqrt{-i} \eta(z)$$

Define $f(z) = \text{const} |\eta(x + iy)| y^{1/4}$

Modular Dedekind η – function is invariant with respect to $SL(2, \mathbb{Z})$ group

$$\eta(z) = e^{\pi iz/12} \prod_{n=0}^{\infty} (1 - e^{2\pi inz}); \quad z = x + iy \quad (y > 0)$$

$$\eta(z + 1) = e^{\pi iz/12} \eta(z)$$

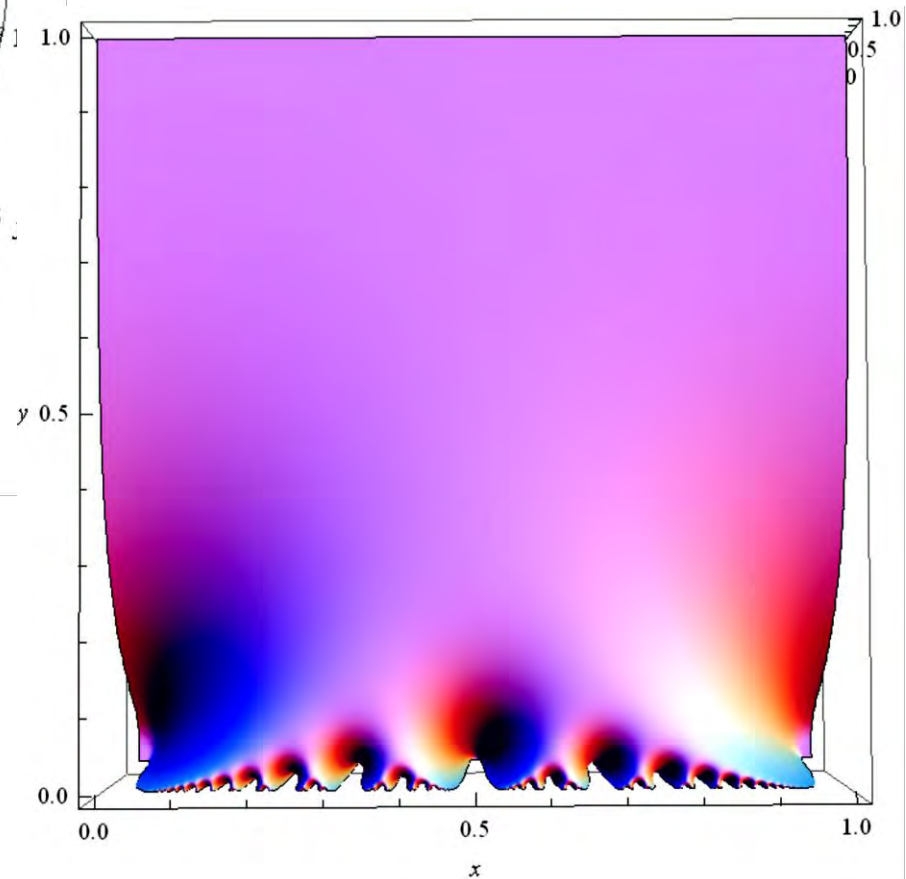
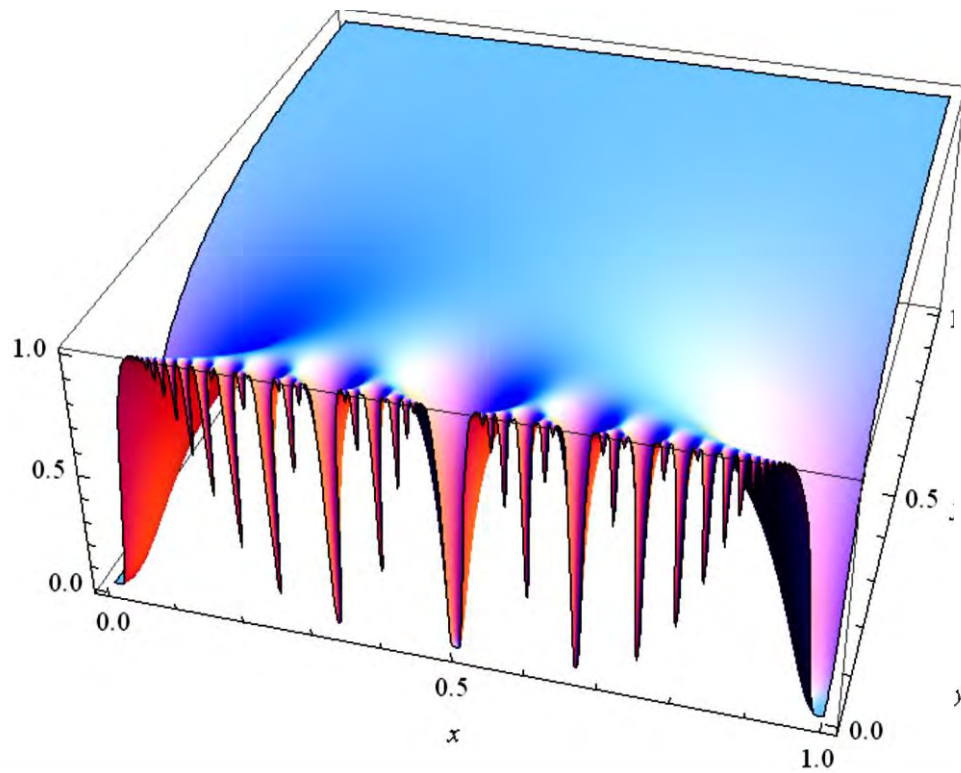
$$\eta\left(-\frac{1}{z}\right) = \sqrt{-i} \eta(z)$$

Define $f(z) = \text{const} |\eta(x + iy)| y^{1/4}$

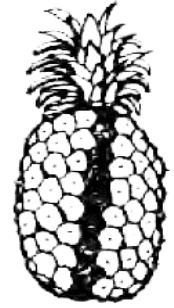
$f(z)$ obeys duality relation

$$f\left(\frac{k}{k+1} + iy\right) = f\left(\frac{1}{k+1} + \frac{i}{(k+1)^2 y}\right)$$

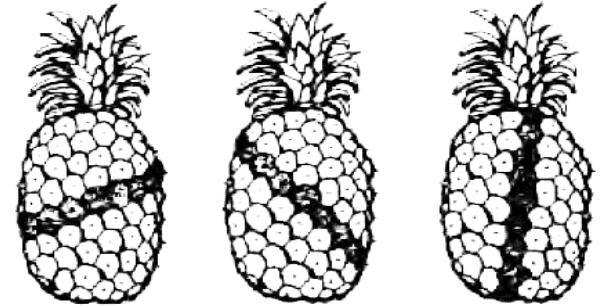
$$f(z) = \text{const} \left| \eta(x + iy) \right| y^{1/4}$$



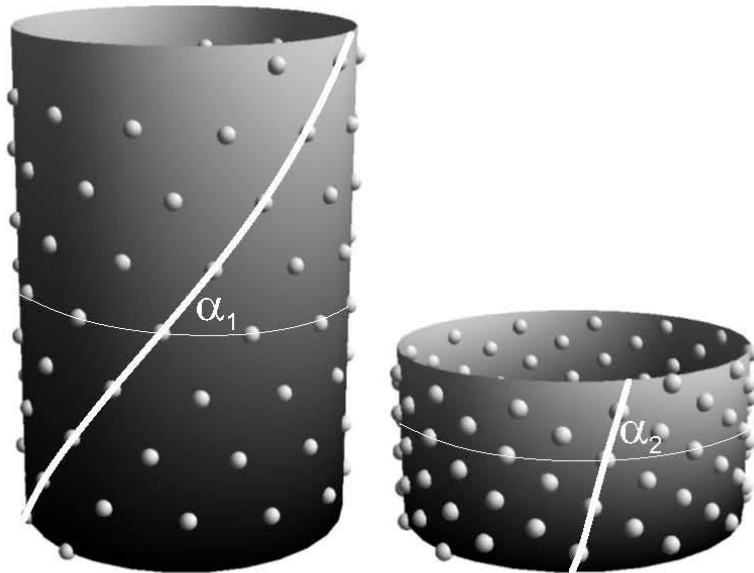
Phyllotaxis



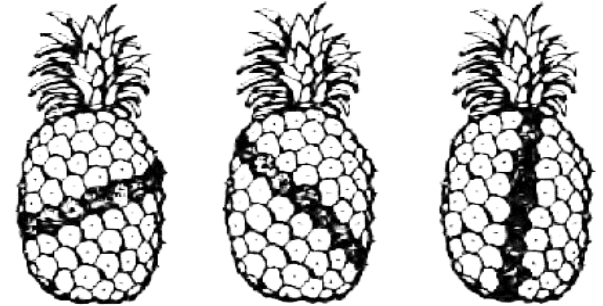
Phyllotaxis



Energetic approach to phyllotaxis, L. Levitov, (1991)



Phyllotaxis

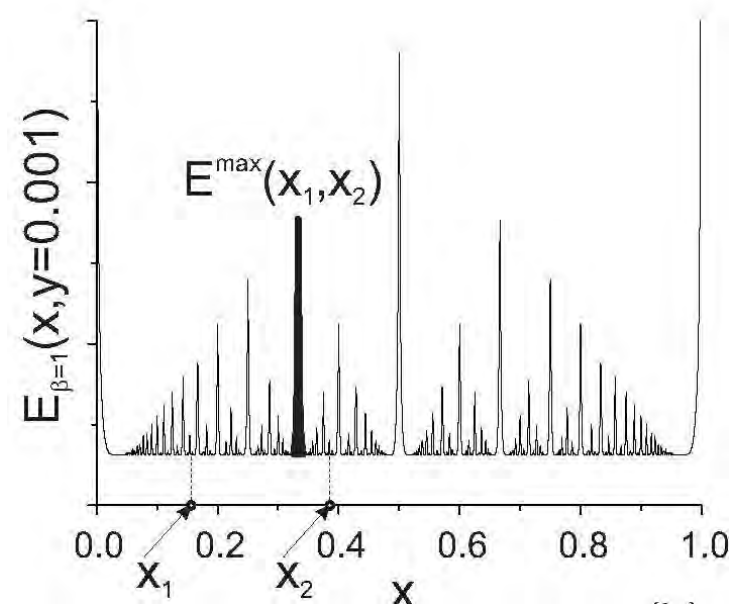
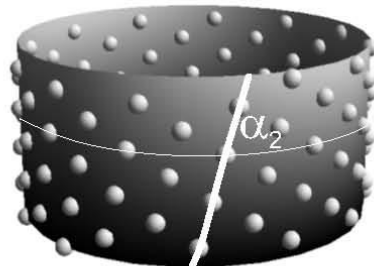
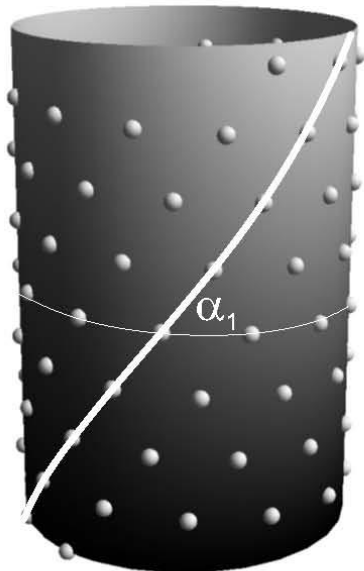


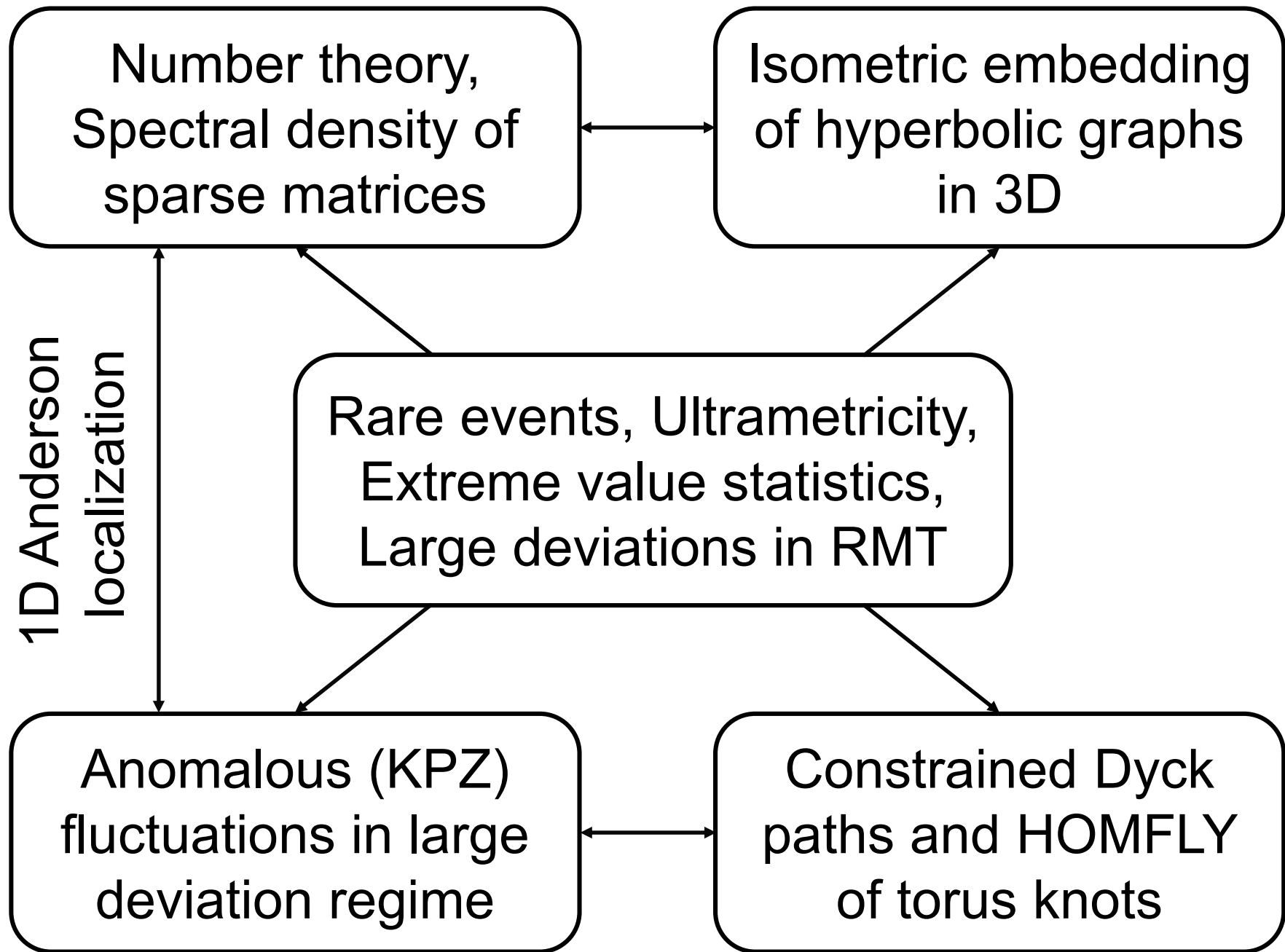
Energetic approach to phyllotaxis, L. Levitov, (1991)

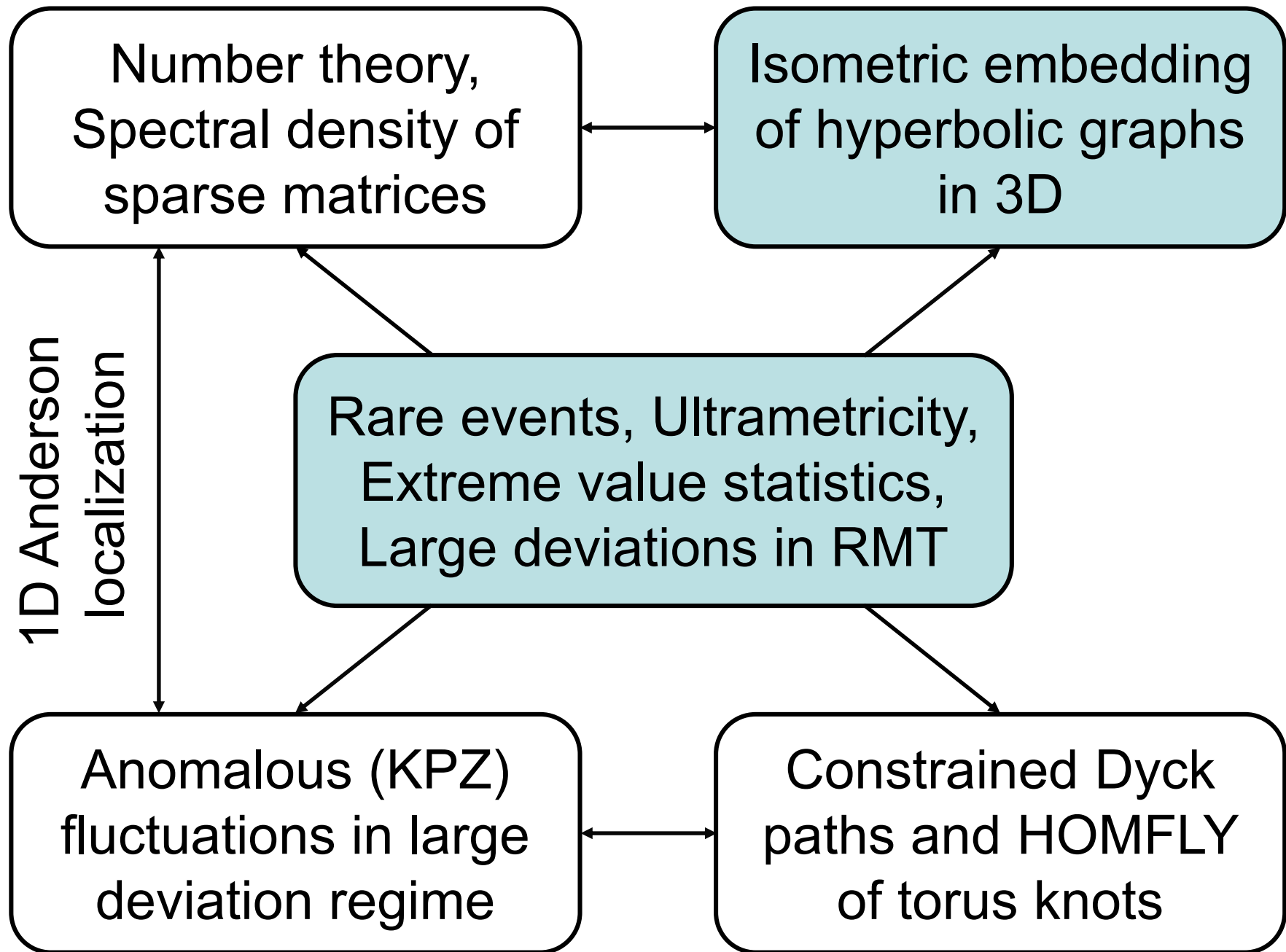
$$x = \frac{\alpha}{2\pi}, \quad y = \frac{h}{2\pi}$$

$$r_{n,m} = \left(\frac{m + nx}{\sqrt{y}}, n\sqrt{y} \right)$$

$$E = \sum_{n,m} e^{-\frac{c(m+nx)^2}{y} - cny^2}$$







Conjectures

- Hierarchical (ultrametric) organization occurs in collective variables when conformational space is huge, and statistics is rare.
- Such a situation is natural for protein folding, analysis of statistical properties of genome, "large data", etc ...
- Another option: ultrametricity occurs as a conflict between intrinsic geometry of object and geometry of space of embedding

Международная конференция

Турбулентность и волновые процессы

Посвященная 100-летию со дня рождения
академика М.Д. Миллионщикова

Москва, 26-28 ноября 2013 г.



Международная конференция

Турбулентность и волновые процессы

Посвященная 100-летию со дня рождения
академика М.Д. Миллионщикова

Москва, 26-28 ноября 2013 г.

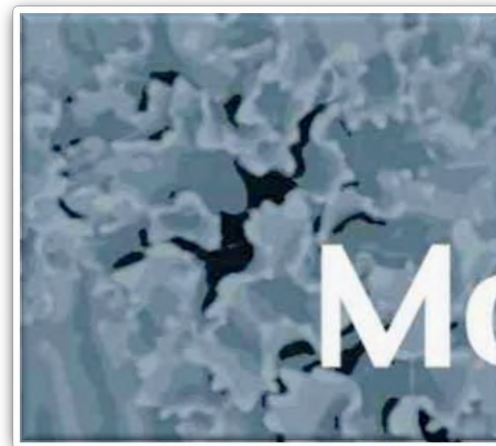
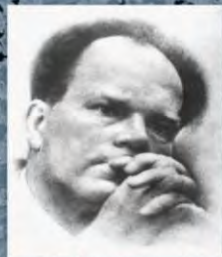


Международная конференция

Турбулентность и волновые процессы

Посвященная 100-летию со дня рождения
академика М.Д. Миллионщикова

Москва, 26-28 ноября 2013 г.



Международная конференция



Турбулентность и волновые процессы

Посвященная 100-летию со дня рождения
академика М.Д. Миллионщикова

Москва, 26-28 ноября 2013 г.



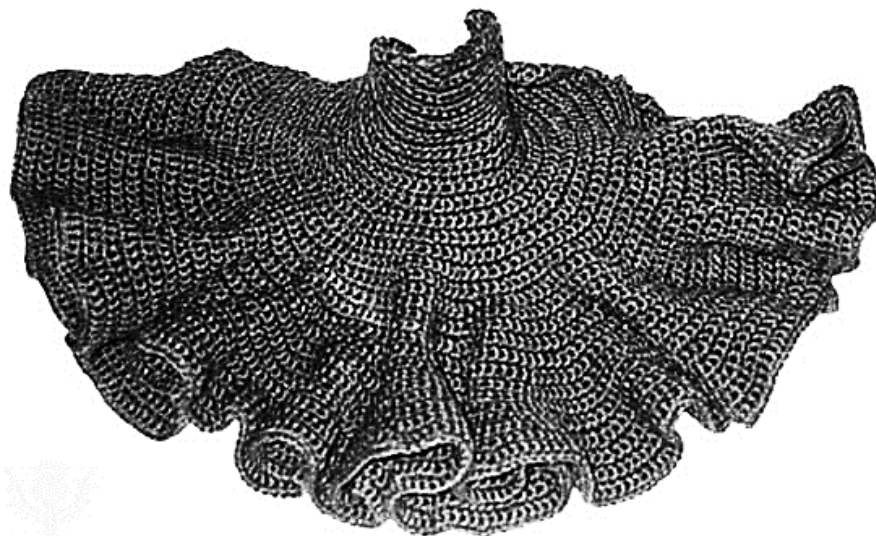
Международная конференция



Турбулентность и волновые процессы

Посвященная 100-летию со дня рождения
академика М.Д. Миллионщикова

Москва, 26-28 ноября 2013 г.



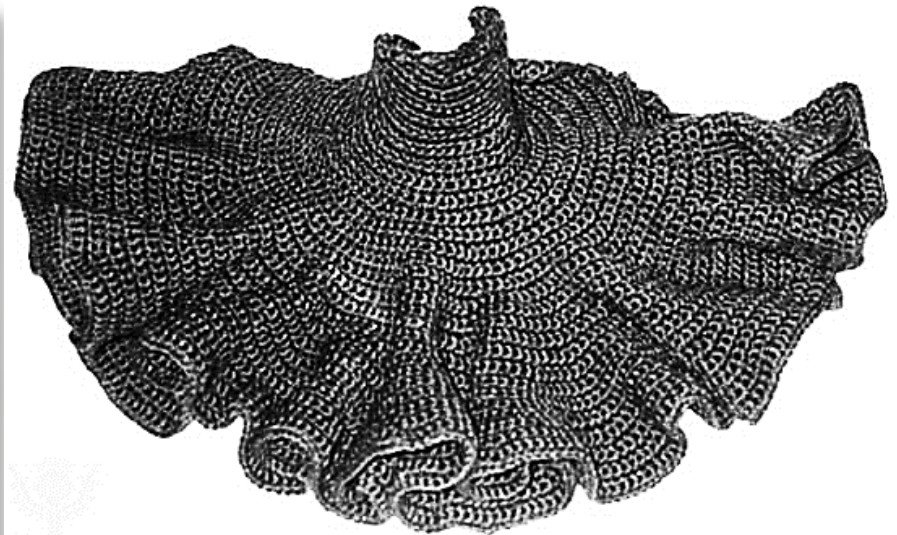
Международная конференция



**Турбулентность
и волновые процессы**

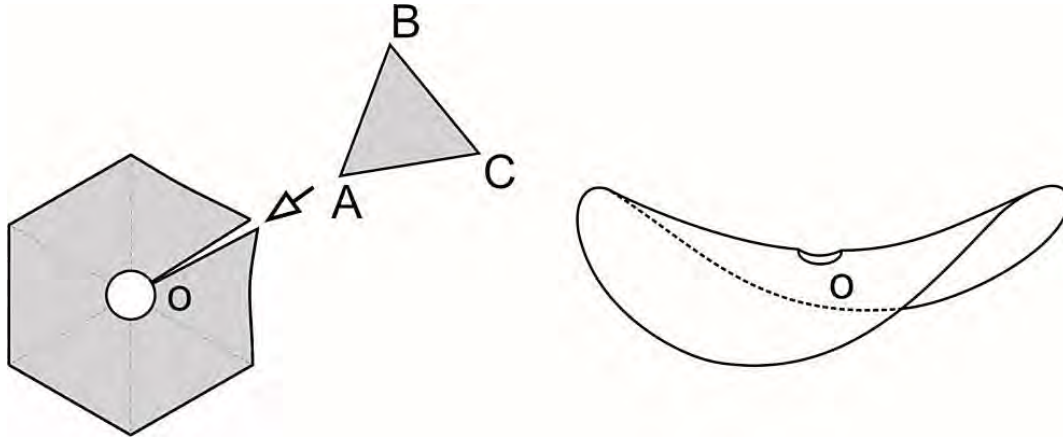
Посвященная 100-летию со дня рождения
академика М.Д. Миллионщикова

Москва, 26-28 ноября 2013 г.

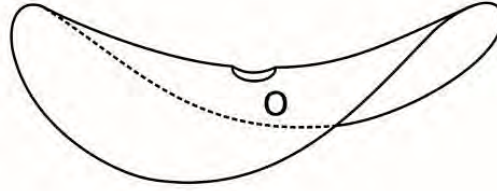
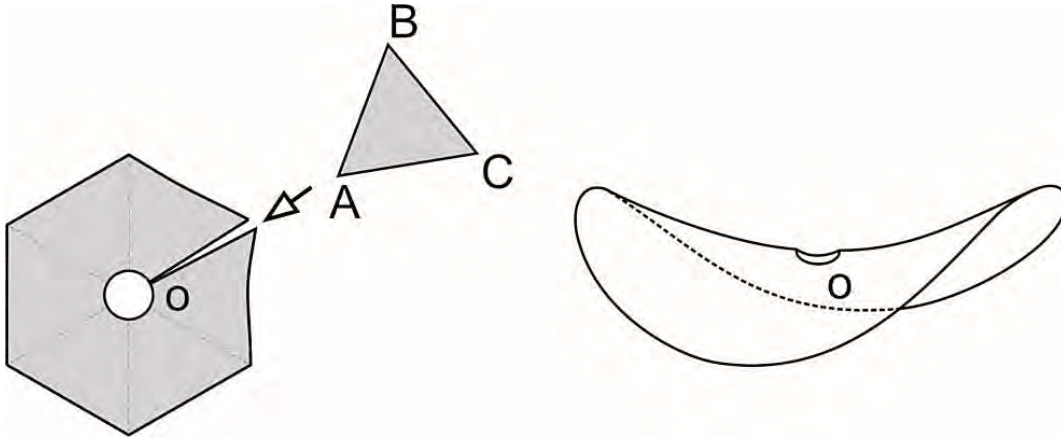


How to describe the profile?

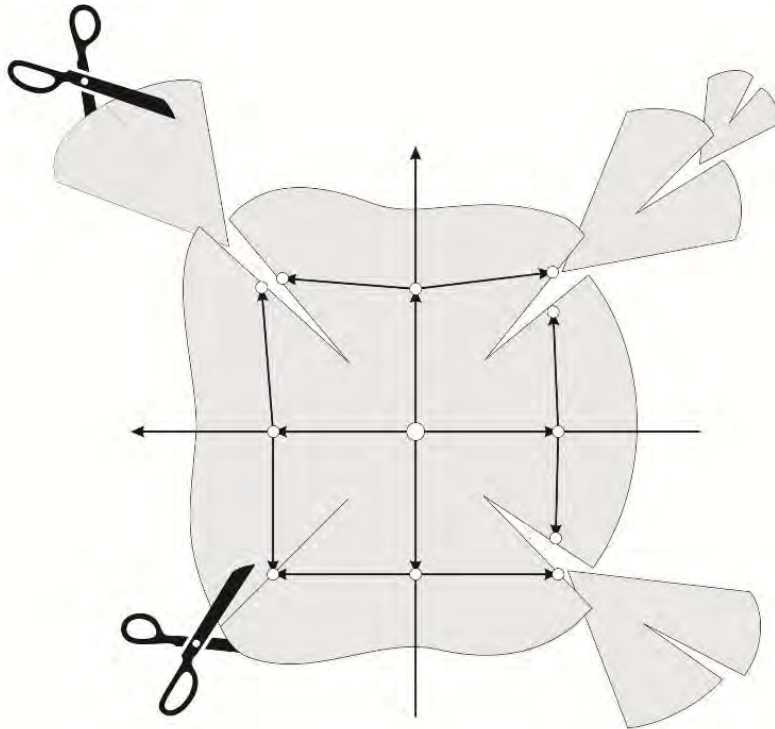
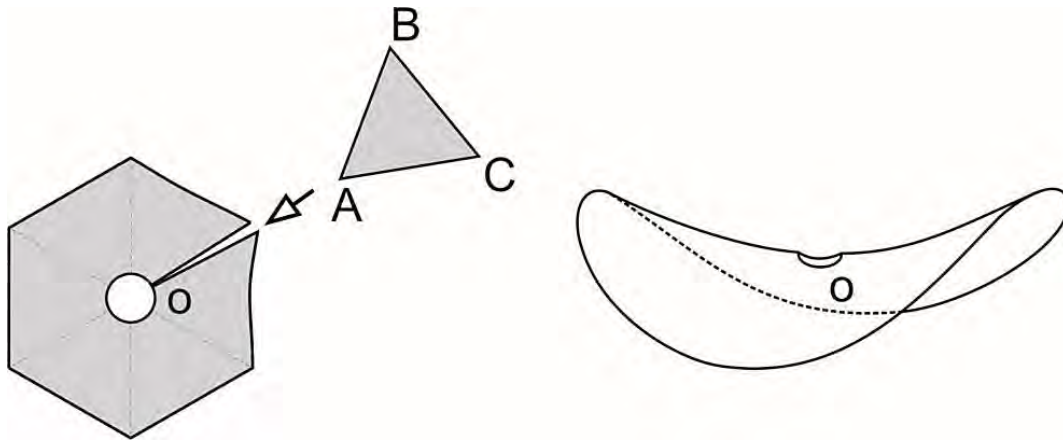
(R. Voituriez, S.N., J. Phys. A, 2001)



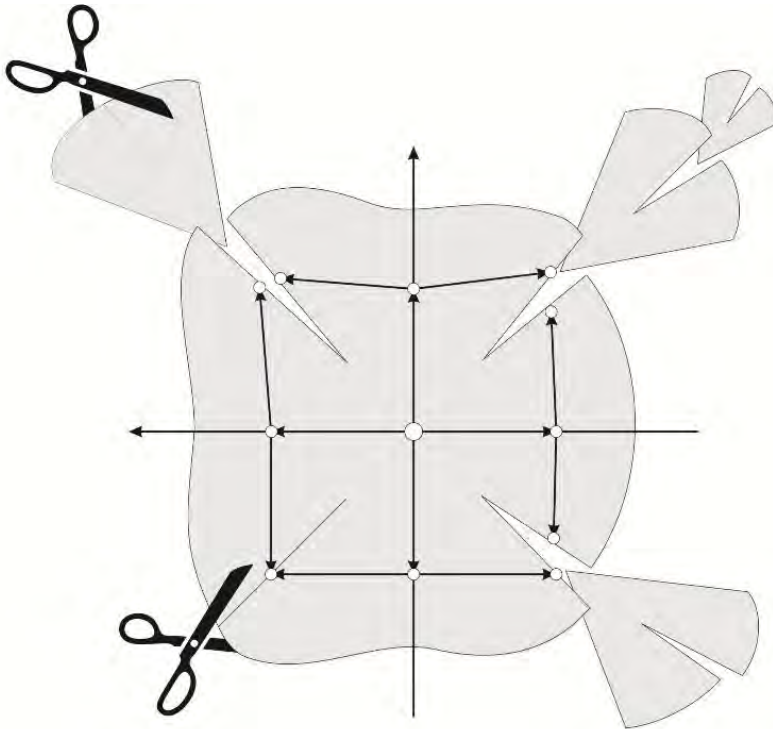
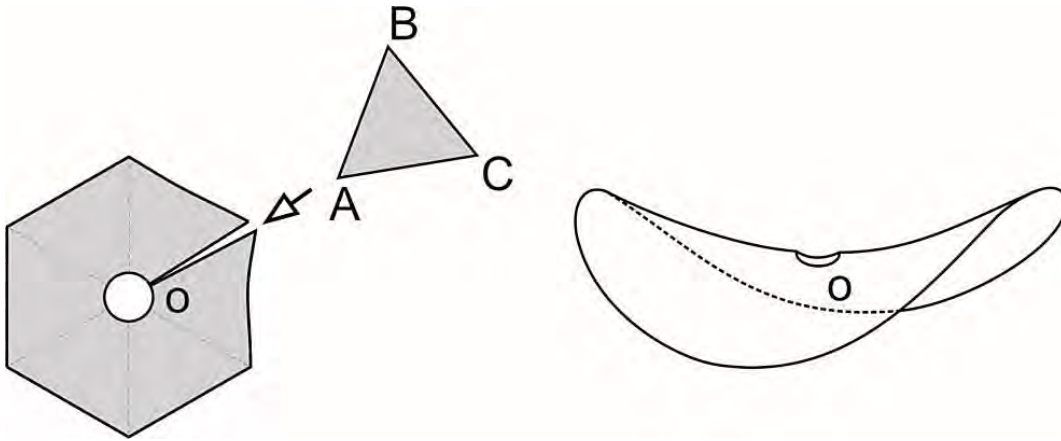
(R. Voituriez, S.N., J. Phys. A, 2001)



(R. Voituriez, S.N., J. Phys. A, 2001)



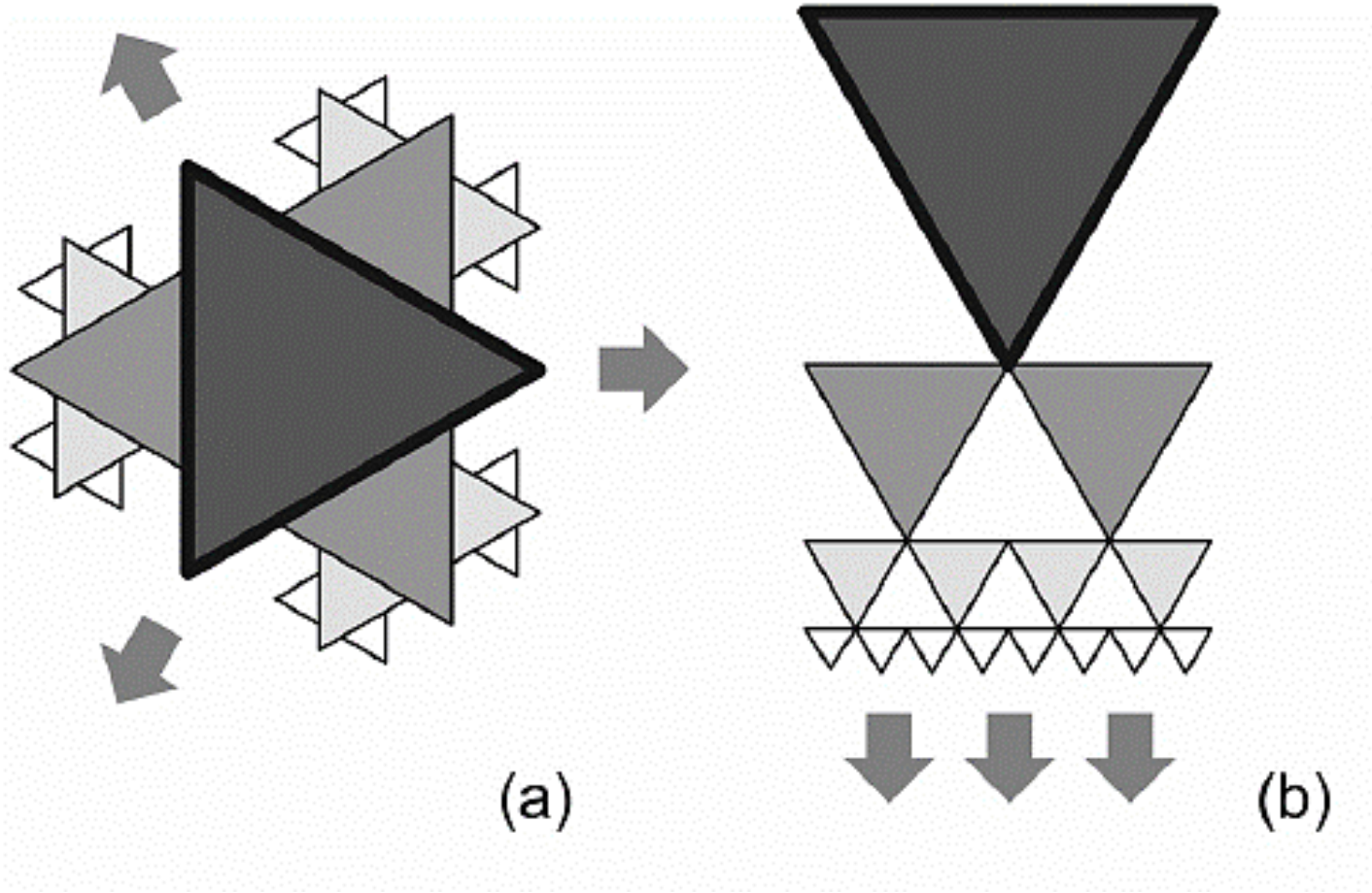
(R. Voituriez, S.N., J. Phys. A, 2001)



Jupe à godets



Exponential proliferation of cells in a thin slit



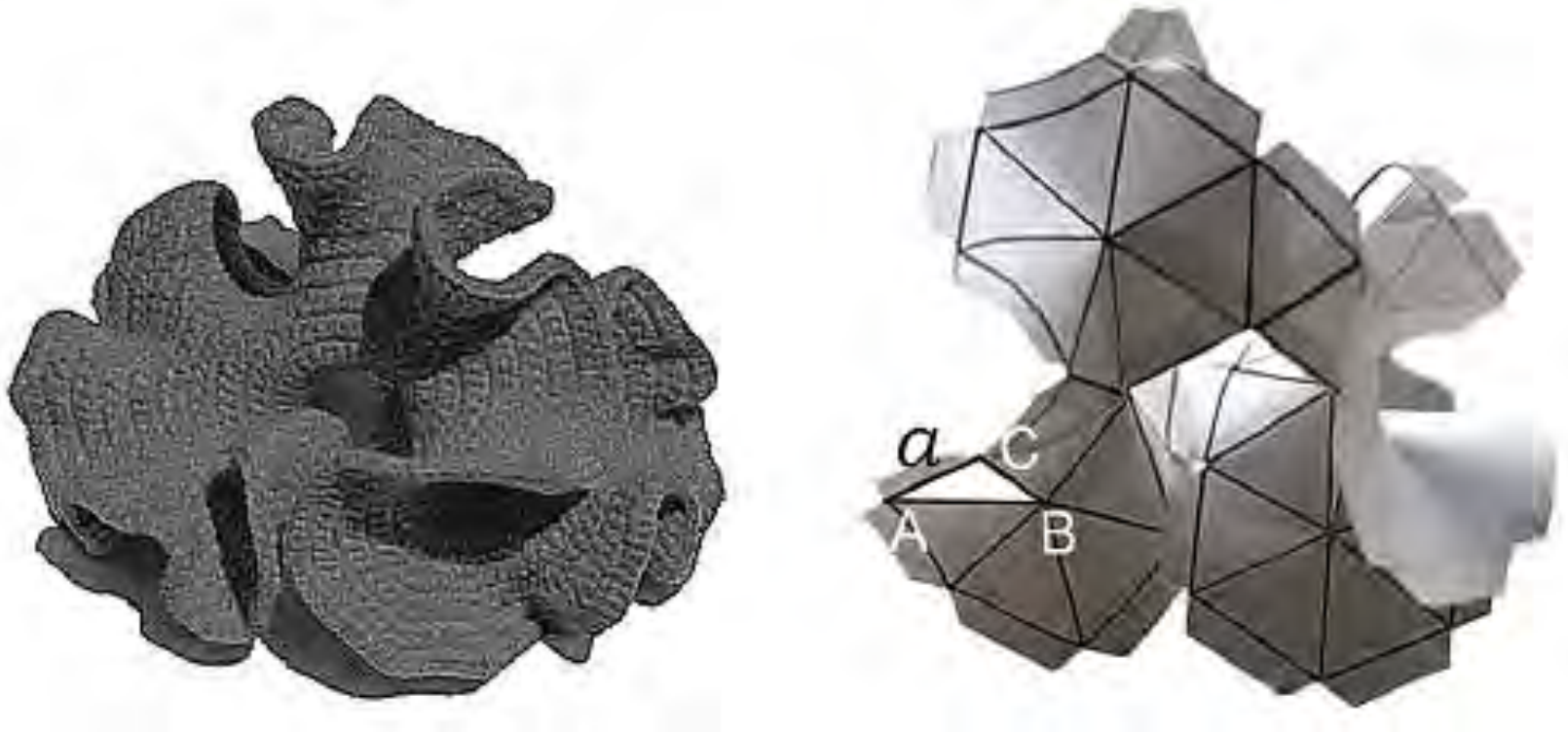
Growth in a disc

Growth in a strip

When we open the slit, the material relaxes into the 3D structure



When we open the slit, the material relaxes into the 3D structure



Buckling occurs as a conflict between intrinsic geometry of object and geometry of space of embedding

Growth induces strain in a tissue near its edge and results in:

- (i) in-plane tissue compression and/or redistribution of layer cells accompanied by the in-plane instability (“stretching”)
- (ii) out-of-plane tissue buckling with the formation of saddle-like surface regions (“bending”)

Growth induces strain in a tissue near its edge and results in:

- (i) in-plane tissue compression and/or redistribution of layer cells accompanied by the in-plane instability (“stretching”)
- (ii) out-of-plane tissue buckling with the formation of saddle-like surface regions (“bending”)

For bending rigidity of a thin membrane $B \sim h^3$, while for stretching rigidity, $S \sim h$, where h is the membrane thickness.

Growth induces strain in a tissue near its edge and results in:

- (i) in-plane tissue compression and/or redistribution of layer cells accompanied by the in-plane instability (“stretching”)
- (ii) out-of-plane tissue buckling with the formation of saddle-like surface regions (“bending”)

For bending rigidity of a thin membrane $B \sim h^3$, while for stretching rigidity, $S \sim h$, where h is the membrane thickness.

Thin tissues, with $h \ll 1$, prefer to bend, i.e. to be negatively curved under relatively small critical strain

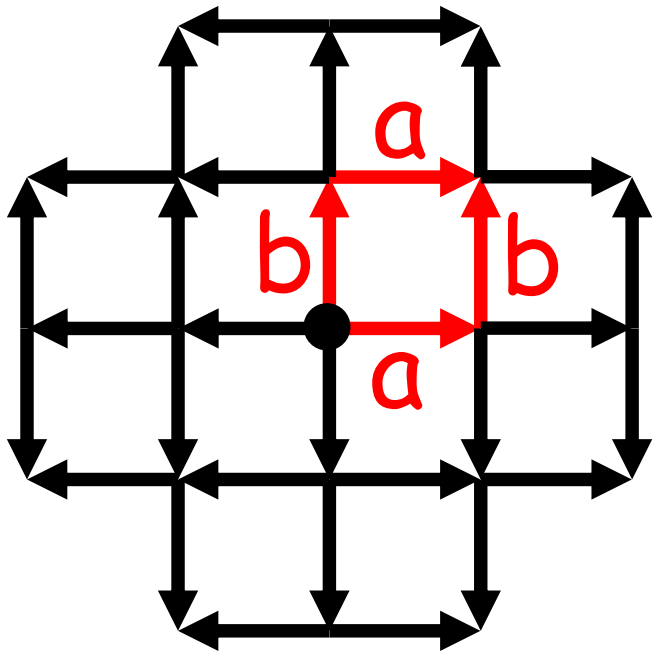
Formulation of the problem

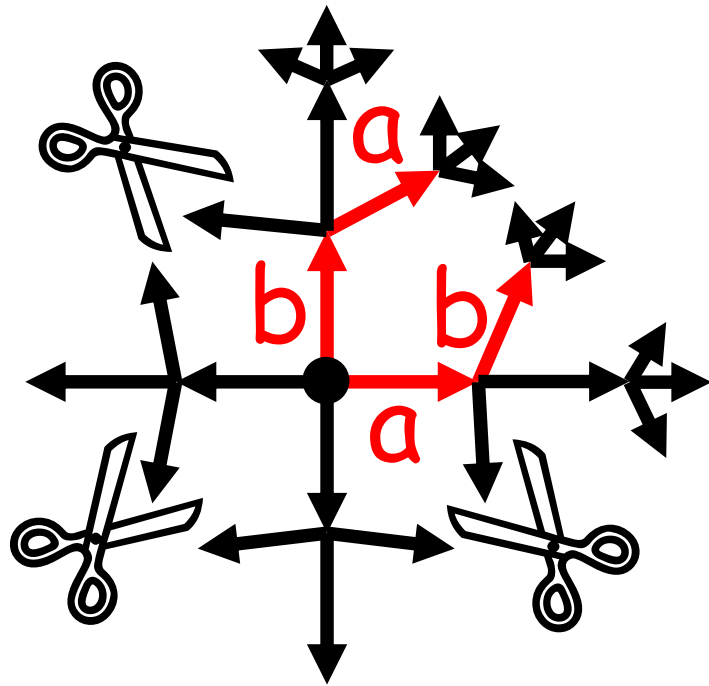
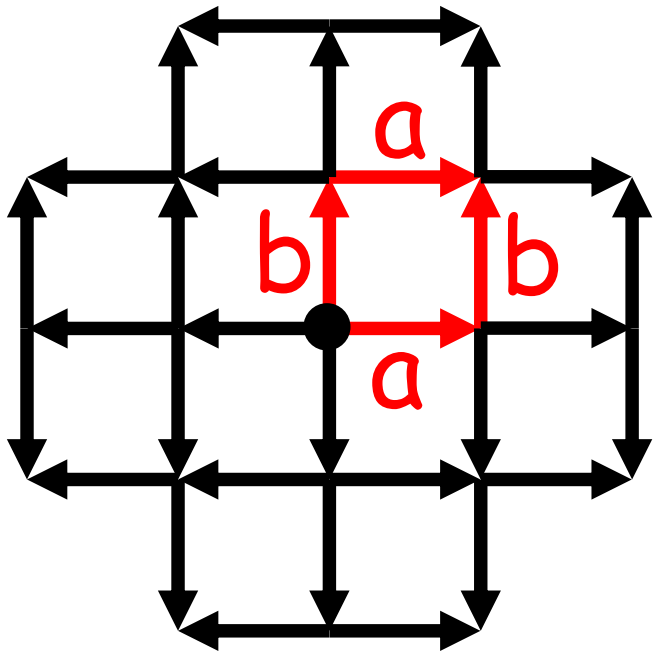
Exponentially growing colony (hyperbolic structure) admits Cayley trees as possible discretizations.

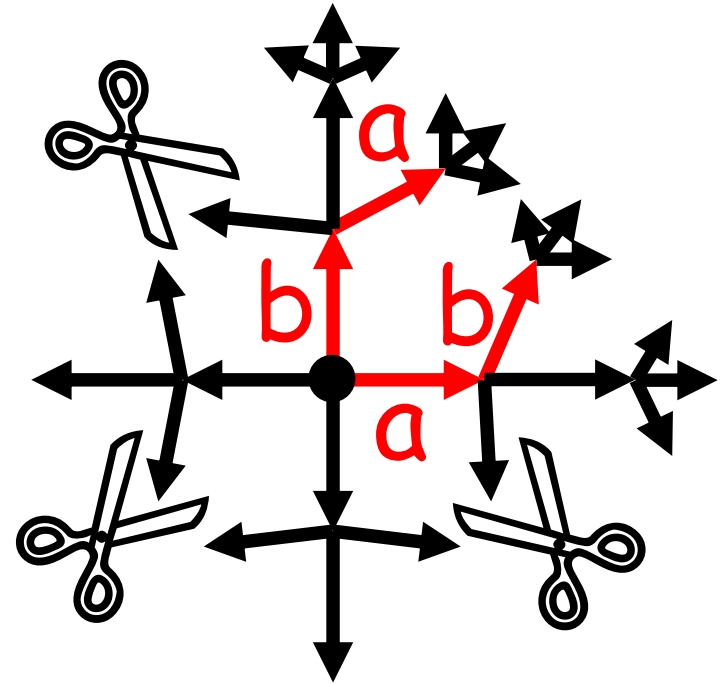
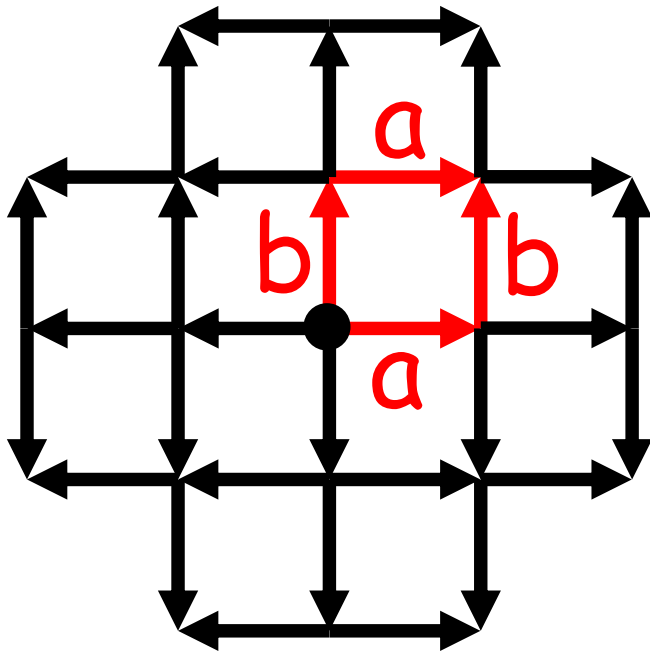
The Cayley trees cover the hyperbolic surface *isometrically*, i.e. without gaps and selfintersections, preserving angles and distances.

Our goal is an embedding a Cayley tree into a 3D Euclidean space with a signature $\{+1,+1,+1\}$.

Hilbert theorem prohibits embedding of unbounded Hyperbolic surface into Euclidean space smoothly



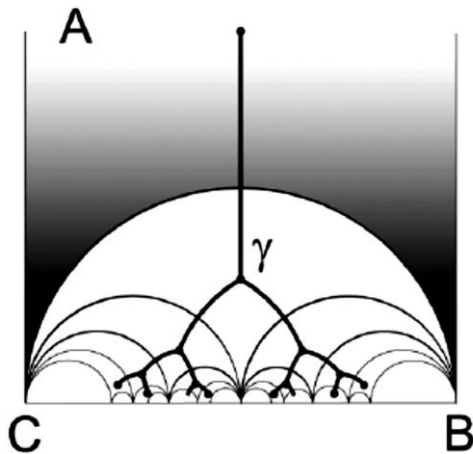
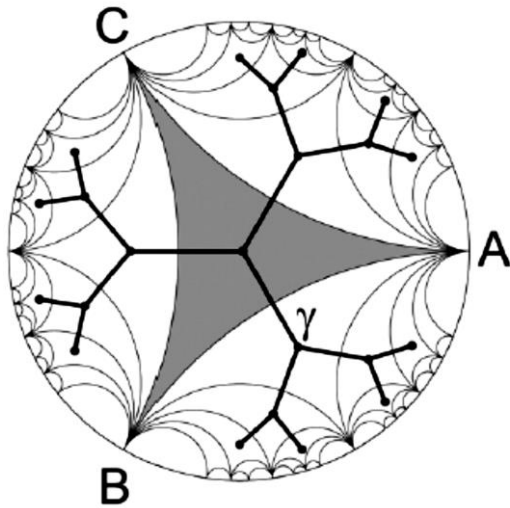




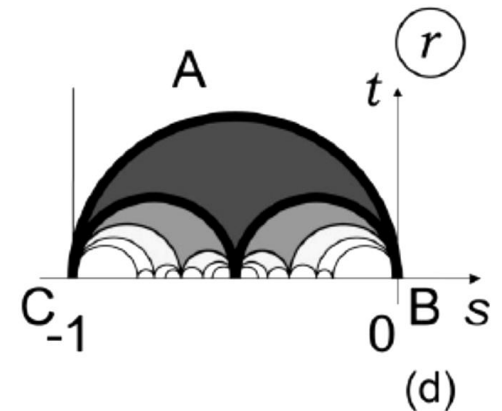
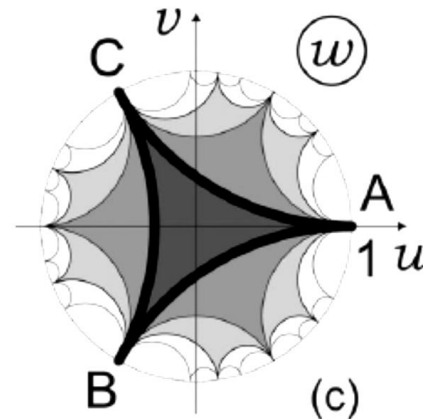
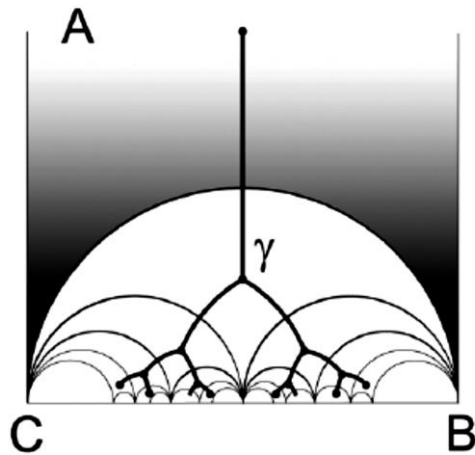
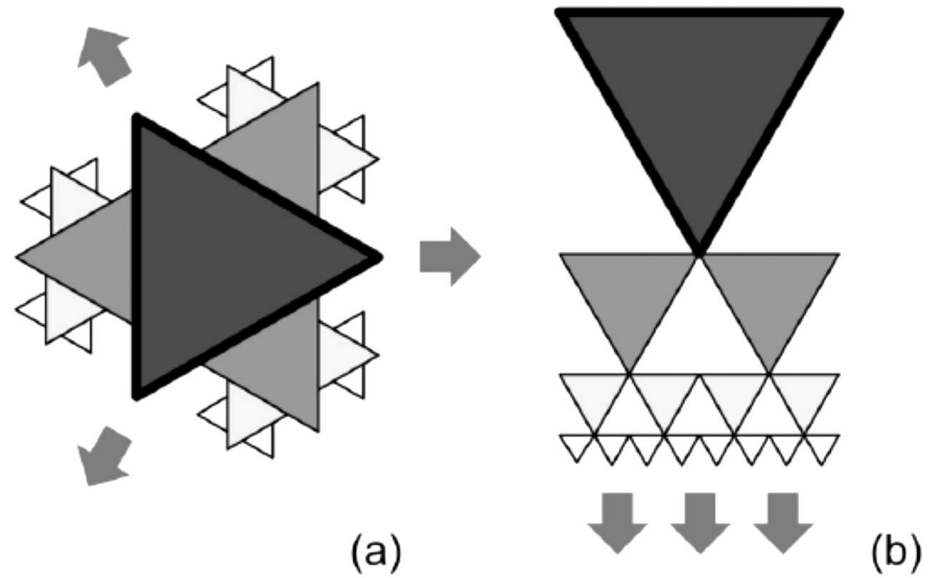
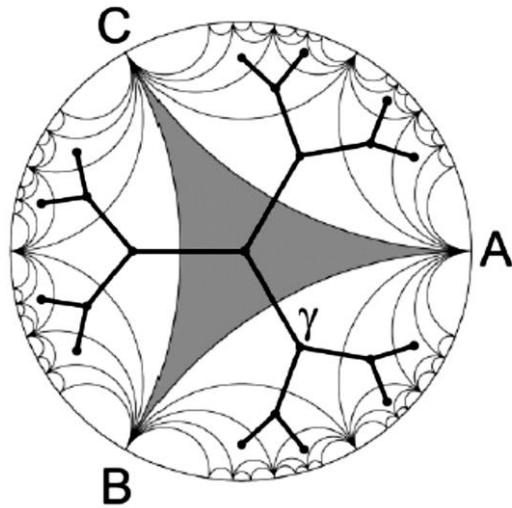
The relief of the surface is encoded in the *coefficient of deformation*, coinciding with the Jacobian $J(\zeta)$ of the conformal transform $z(\zeta)$, where

$$J(\zeta) = |dz / d\zeta|^2$$

Isometric embedding of a Cayley tree into Poincare disc and a strip

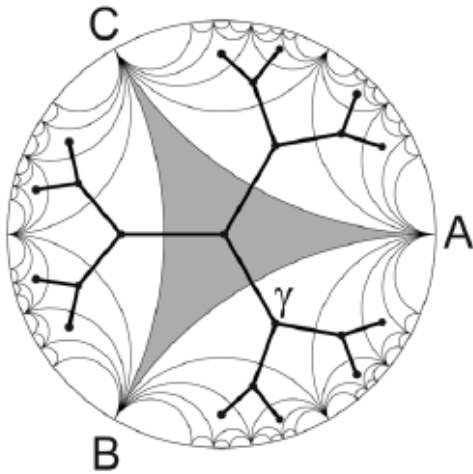


Isometric embedding of a Cayley tree into Poincare disc and a strip



Optimal profile – is the surface in which we can *isometrically* embed exponentially growing graph

(S. N., K. Polovnikov, Soft Matter, 2017)



The metric ds^2 of a 2D surface parametrized by (u, v) , is given by the coefficients

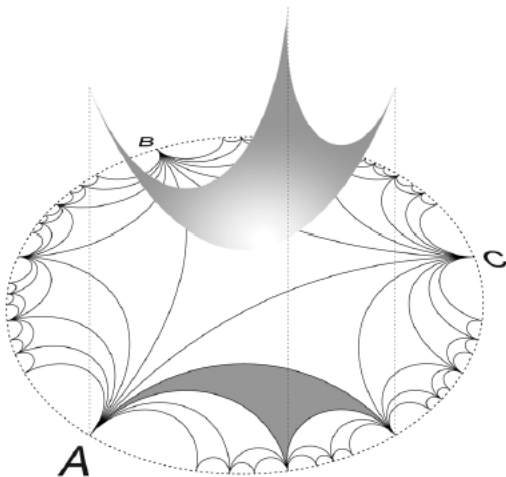
$$E = \mathbf{r}_u^2, \quad G = \mathbf{r}_v^2, \quad F = (\mathbf{r}_u, \mathbf{r}_v)$$

of the first quadratic form of this surface

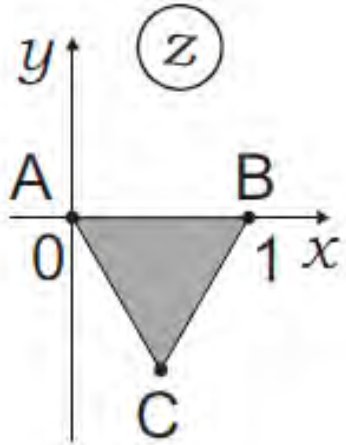
$$ds^2 = Edu^2 + 2F dudv + Gdv^2$$

The surface area then reads

$$dS = \sqrt{EG - F^2} dudv.$$

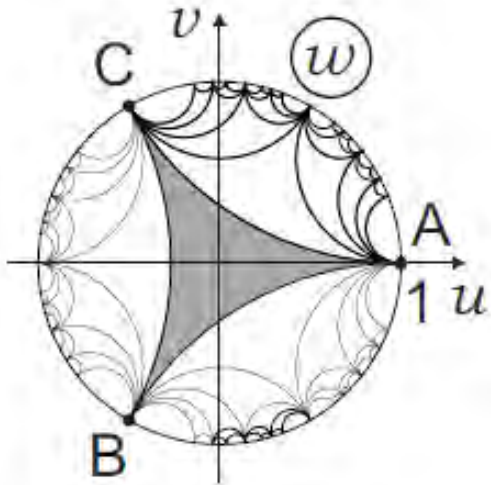


Surface embedded in 3D has the same metric as Poincare disc



$$S_{ABC} = \int_{\Delta ABC} dx dy = \text{const}$$

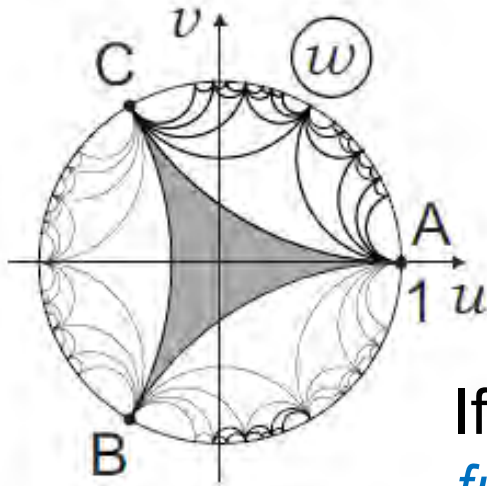
$$S_{ABC} = \int_{\Delta ABC} |J(z, w)| du dv; \quad J(z, w) = \begin{vmatrix} \partial_u x & \partial_u y \\ \partial_v x & \partial_v y \end{vmatrix}$$



If $z(w)$ is holomorphic, the Cauchy-Riemann conditions provide

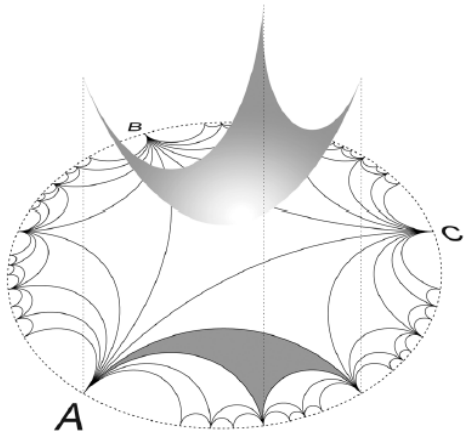
$$J(w) = \left| \frac{dz(w)}{dw} \right|^2 \equiv |z'(w)|^2$$

Surface embedded in 3D has the same metric as Poincare disc



$$S_{A'} = \int_{\Delta A'} |J(z, w)| du dv$$

If we impose the condition for a surface to be a *function* above (u, v) , then we can write the surface element in curvilinear coordinates



$$J(w) = \sqrt{1 + \left(\frac{\partial f}{\partial u}\right)^2 + \left(\frac{\partial f}{\partial v}\right)^2}$$

$$\left(\frac{\partial f(u, v)}{\partial u}\right)^2 + \left(\frac{\partial f(u, v)}{\partial v}\right)^2 = \left|\frac{dz(w)}{dw}\right|^4 - 1$$

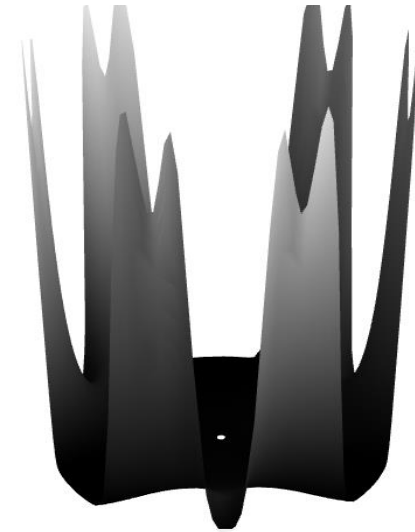
Relief of the surface $f(u, v)$ is defined by the *eikonal* equation

$$\left(\frac{\partial f(u, v)}{\partial u} \right)^2 + \left(\frac{\partial f(u, v)}{\partial v} \right)^2 = \left| \frac{dz(w)}{dw} \right|^4 - 1$$

Relief of the surface $f(u, v)$ is defined by the *eikonal* equation

$$\left(\frac{\partial f(u, v)}{\partial u}\right)^2 + \left(\frac{\partial f(u, v)}{\partial v}\right)^2 = \left|\frac{dz(w)}{dw}\right|^4 - 1$$

In our case we have to solve the equation for the function $f(u, v)$ given by the conformal transform



$$\left(\frac{\partial f(u, v)}{\partial u}\right)^2 + \left(\frac{\partial f(u, v)}{\partial v}\right)^2 = \frac{\alpha^{-2} |\eta(w)|^{16}}{\pi^{4/3} B^4(\frac{1}{3}, \frac{1}{3})} - 1$$

Geometric optic analogy

Comparing equation

$$\left(\frac{\partial f(u, v)}{\partial u}\right)^2 + \left(\frac{\partial f(u, v)}{\partial v}\right)^2 = \frac{a^{-2} |\eta(w)|^{16}}{\pi^{4/3} B^4(\frac{1}{3}, \frac{1}{3})} - 1$$

to the standard eikonal equation for the rays in optically inhomogeneous media

$$(\nabla S)^2 = n^2(x)$$

We conclude that the rays **propagate along optimal Fermat paths** in Euclidean domain. They are projections of geodesics of corresponding “eikonal surface”. The refraction coefficient in this case reads

$$n^2 = |z'(w)|^4 - 1$$

Rigid and flexible circular surfaces

The rigidity in our geometric approach is controlled by the parameter a – the size of elementary flat domain

Rigid and flexible circular surfaces

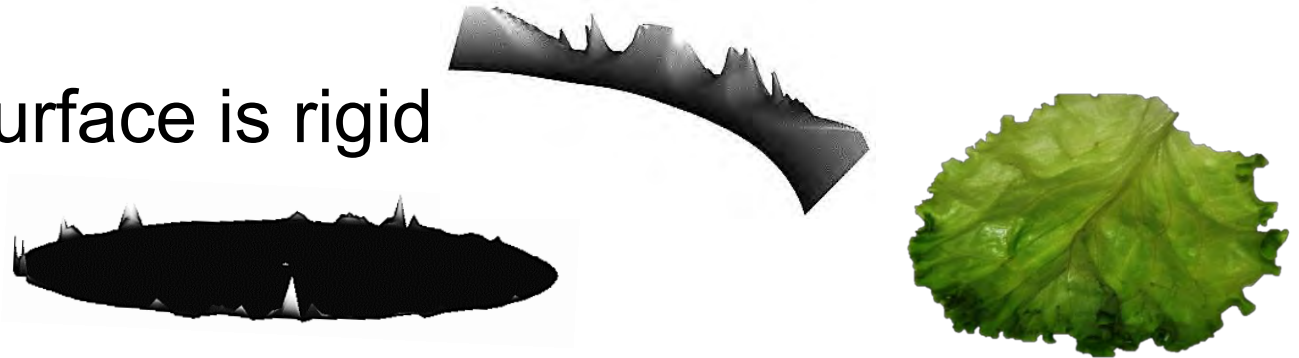
The rigidity in our geometric approach is controlled by the parameter a – the size of elementary flat domain

1) If $a \geq 1$, the surface is rigid

Rigid and flexible circular surfaces

The rigidity in our geometric approach is controlled by the parameter a – the size of elementary flat domain

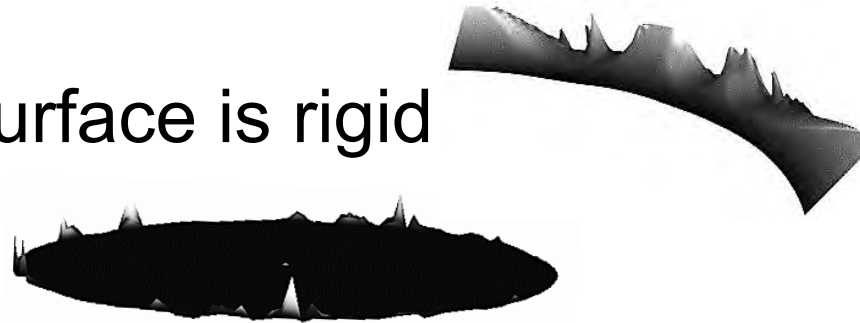
1) If $a \geq 1$, the surface is rigid



Rigid and flexible circular surfaces

The rigidity in our geometric approach is controlled by the parameter a – the size of elementary flat domain

1) If $a \geq 1$, the surface is rigid

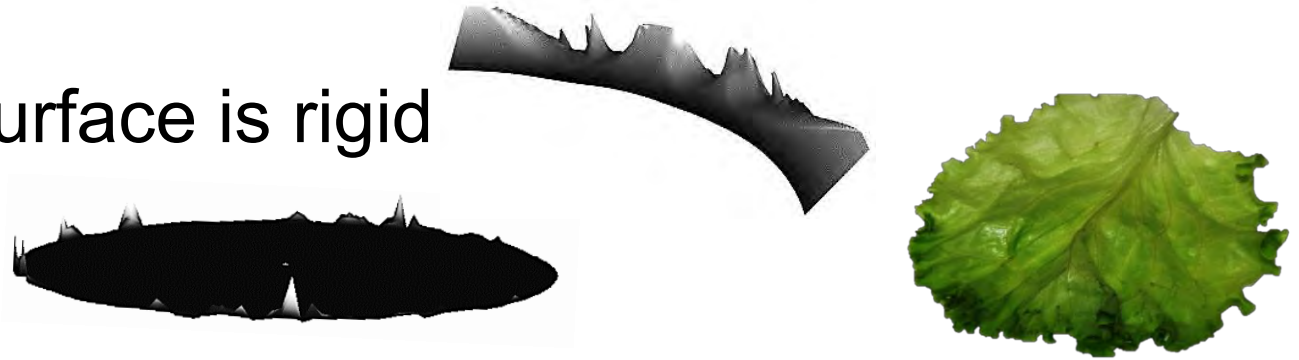


2) If $0 < a \ll 1$, the surface is flexible

Rigid and flexible circular surfaces

The rigidity in our geometric approach is controlled by the parameter a – the size of elementary flat domain

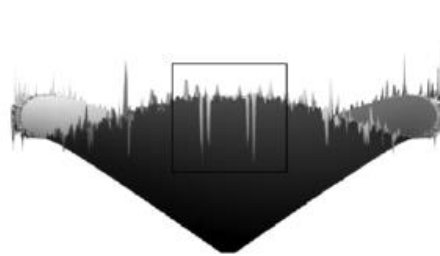
1) If $a \geq 1$, the surface is rigid



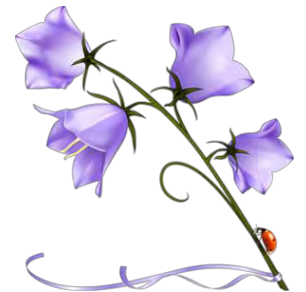
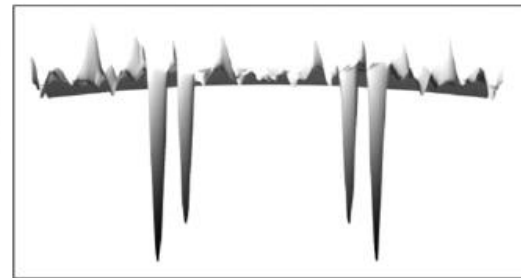
2) If $0 < a \ll 1$, the surface is flexible



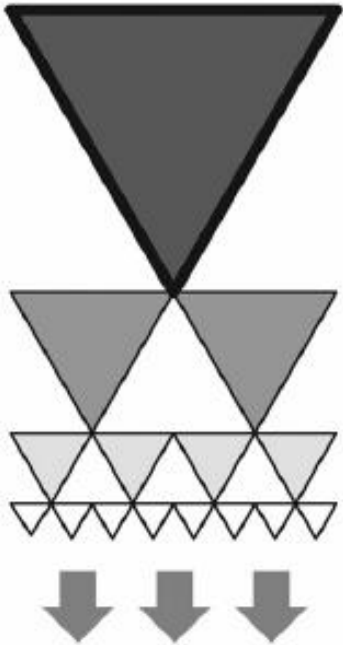
$a=0.07$



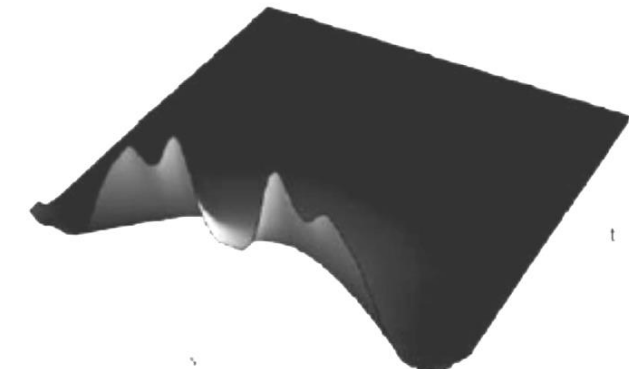
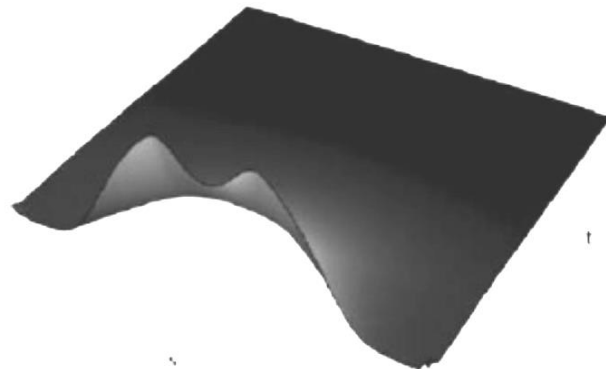
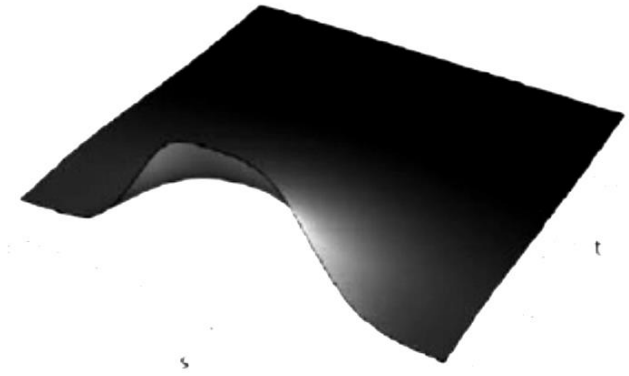
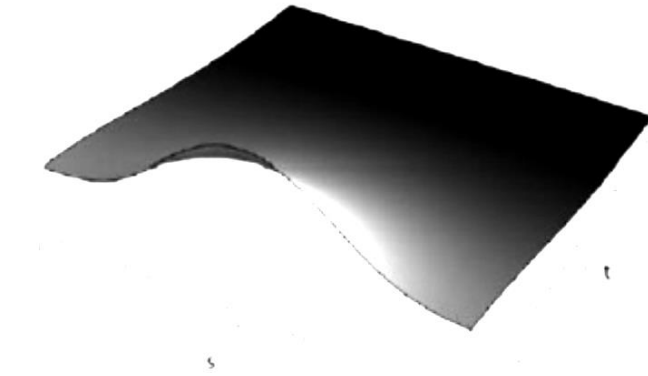
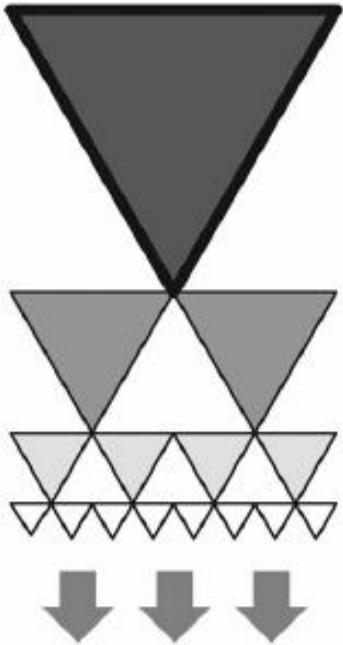
$a=0.14$



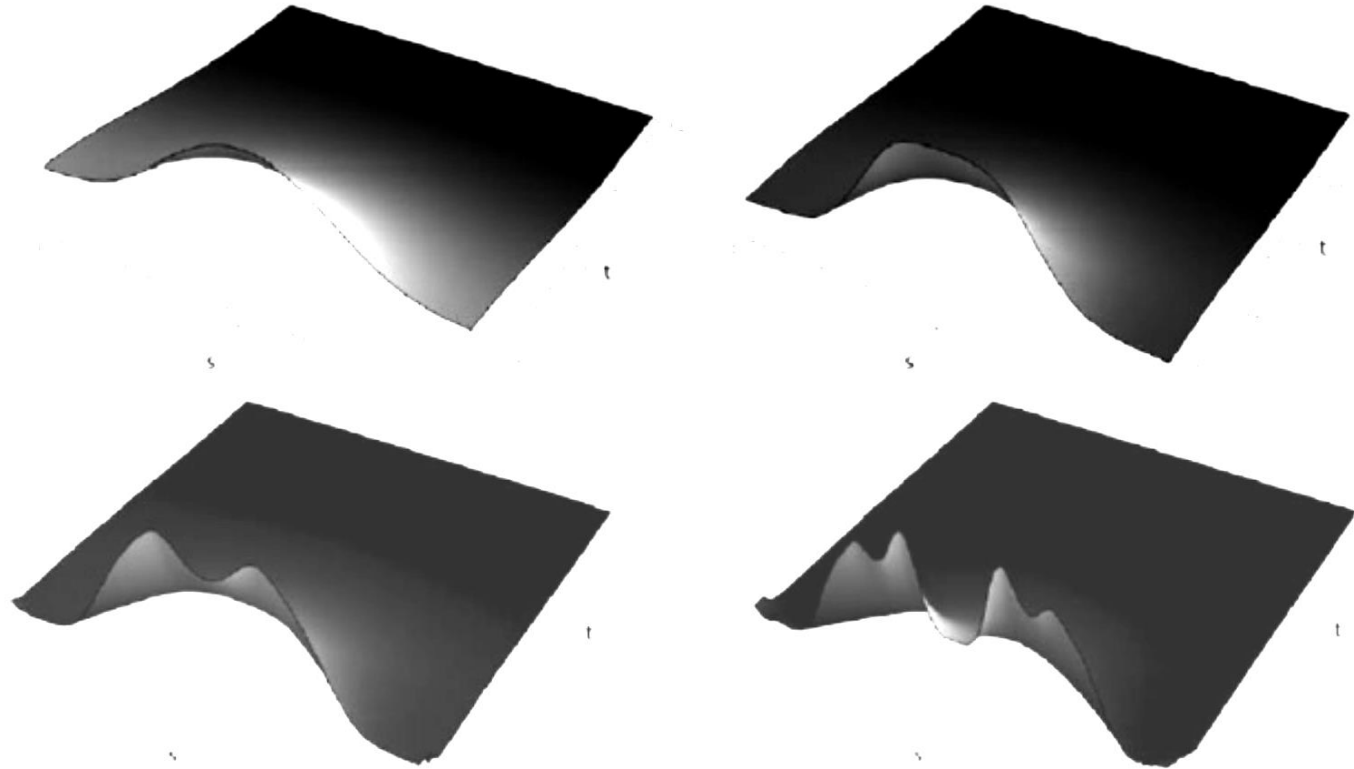
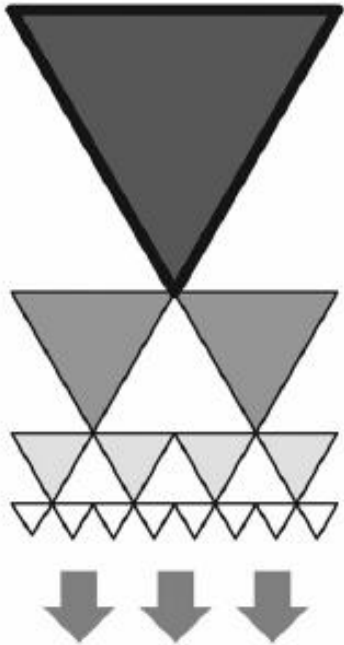
Buckling in a strip



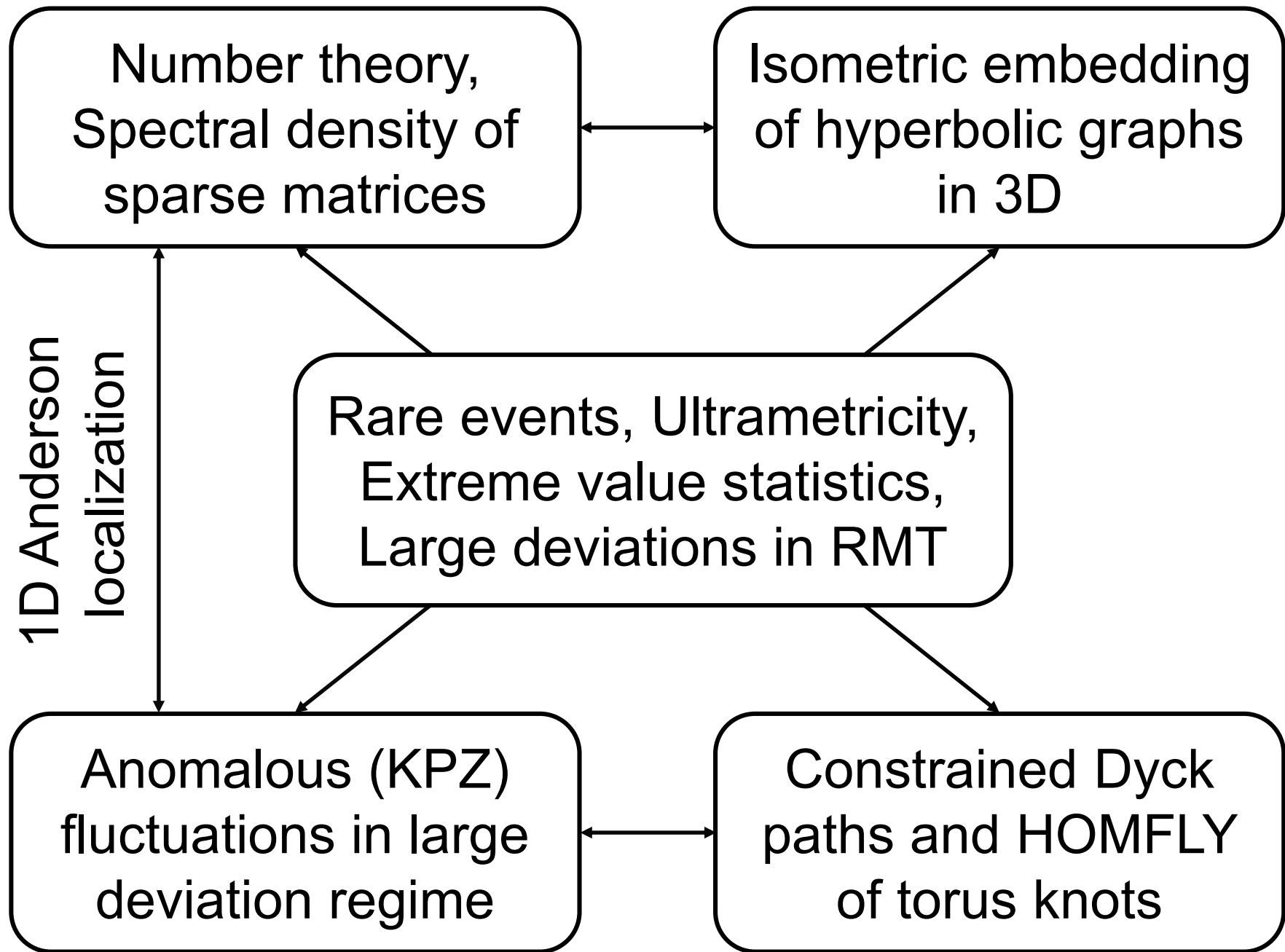
Buckling in a strip

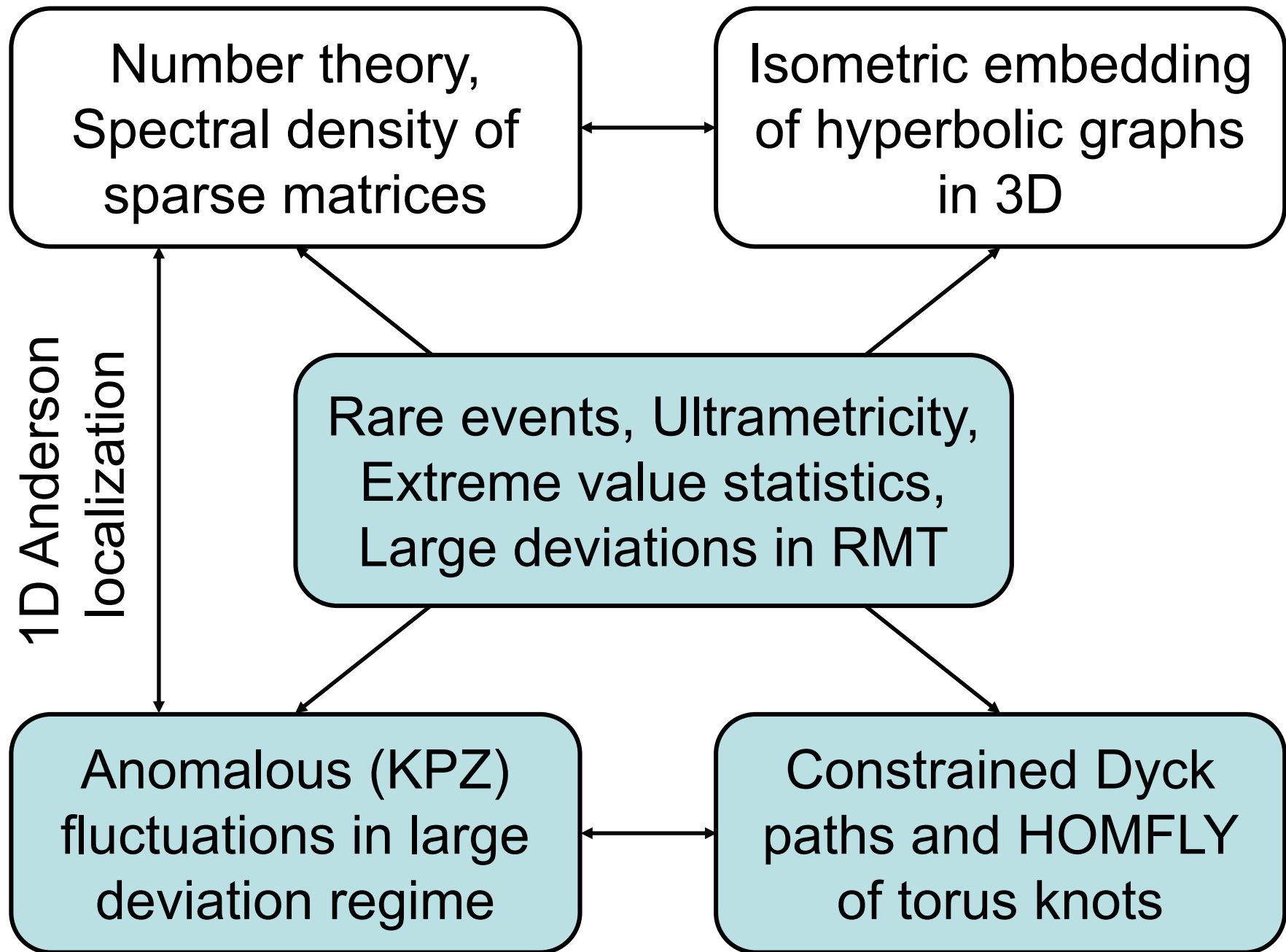


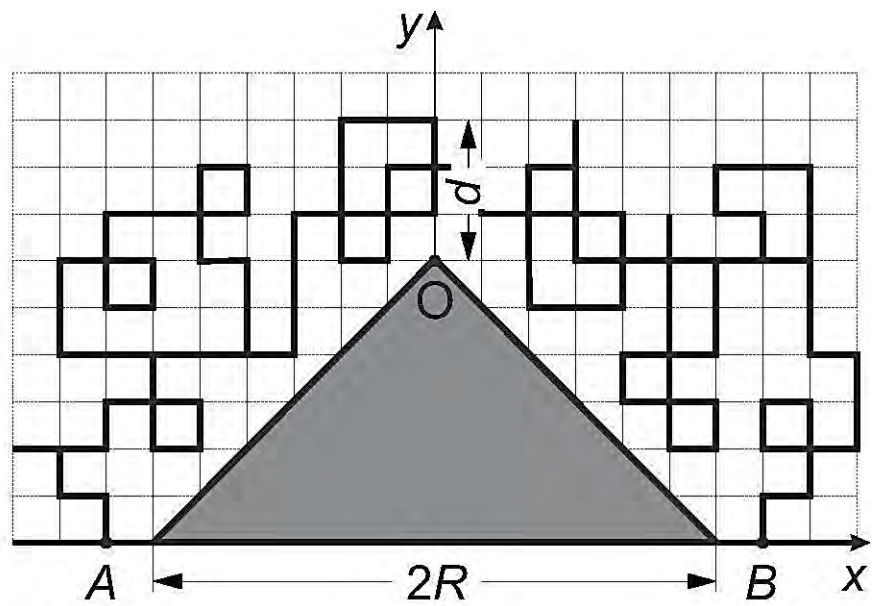
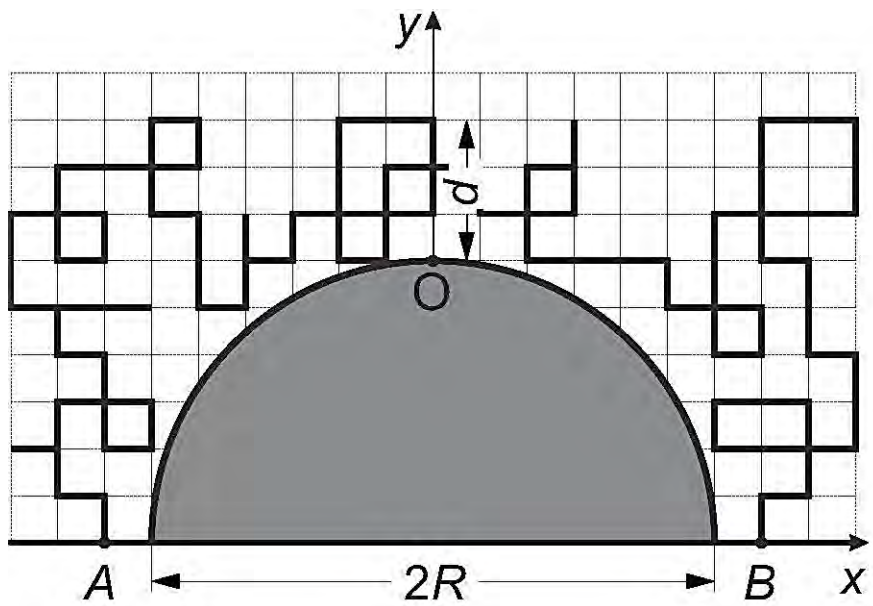
Buckling in a strip

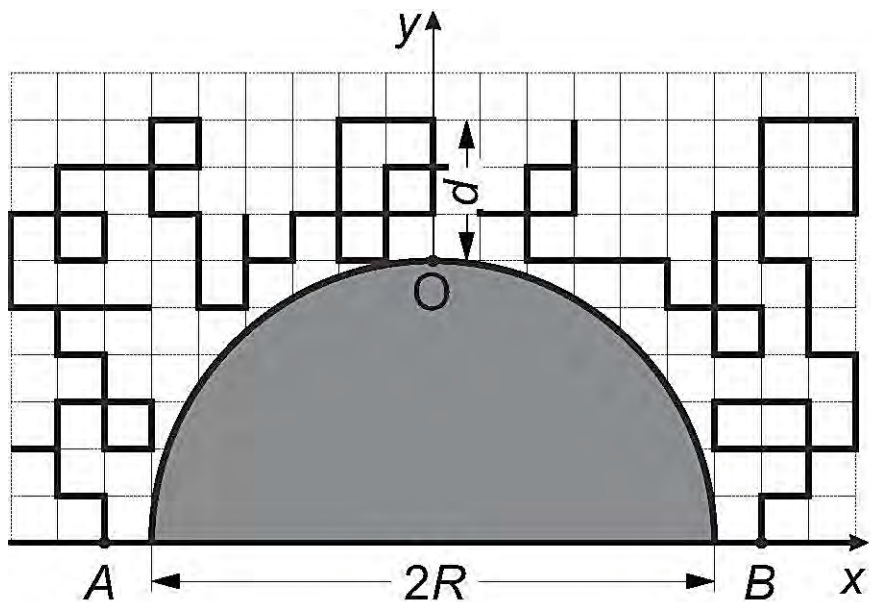


Formation of hierarchical folds due to ultrametricity of Dedekind η -function



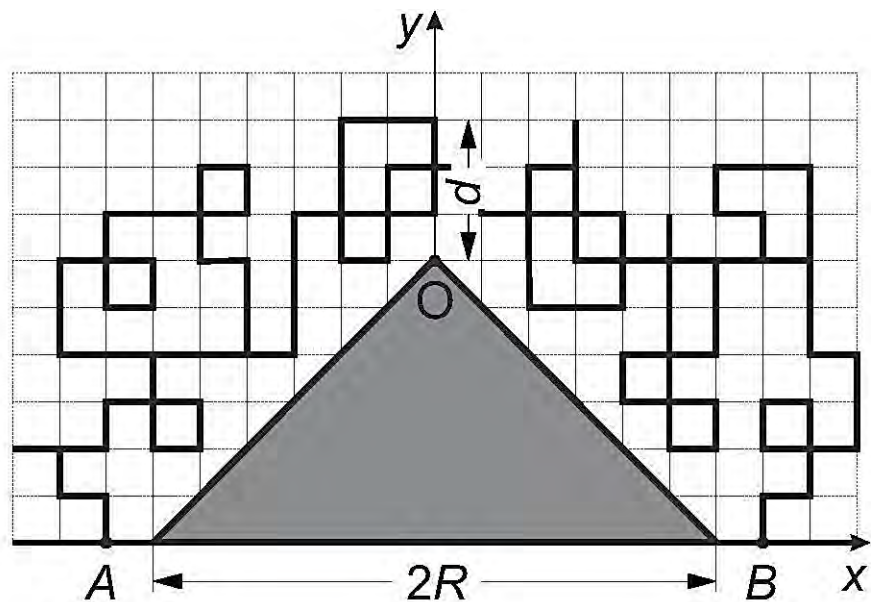






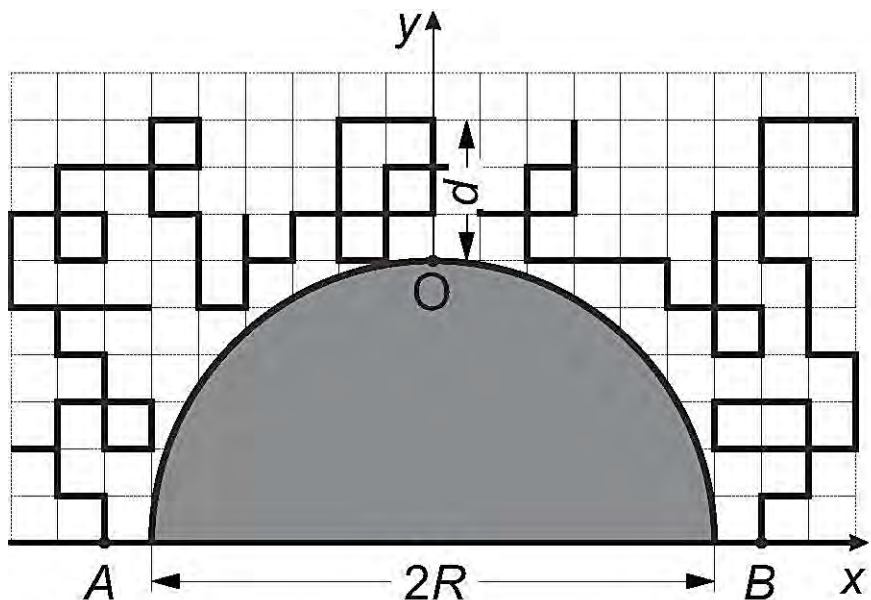
stretched paths
above semicircle

$$\langle d \rangle \sim R^{1/3}$$



stretched paths
above triangle

$$\langle d \rangle = \text{const}$$

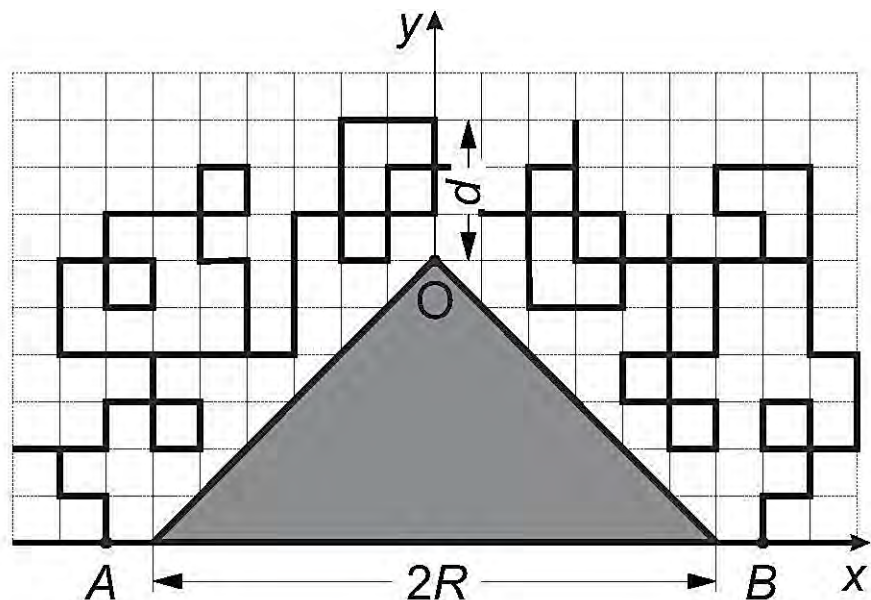


stretched paths
above semicircle

$$\langle d \rangle \sim R^{1/3}$$

For a curve of order γ

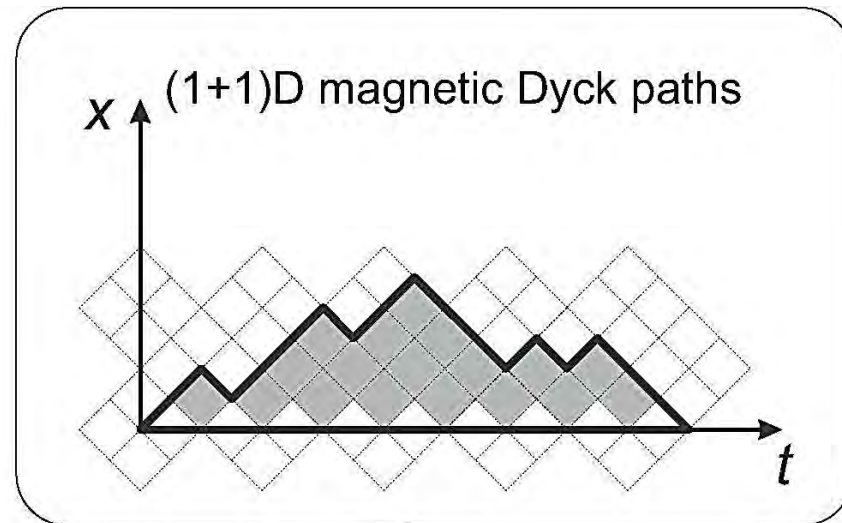
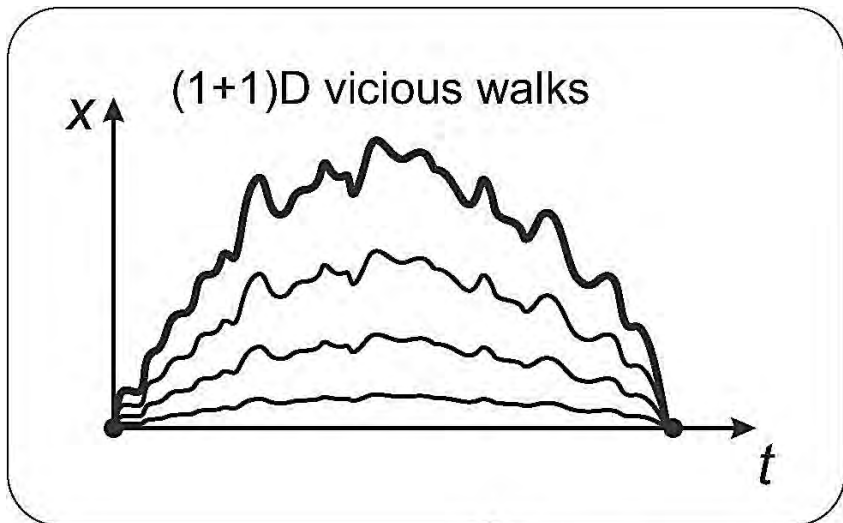
$$\frac{y}{R} = \left(\frac{x}{R} \right)^\gamma$$



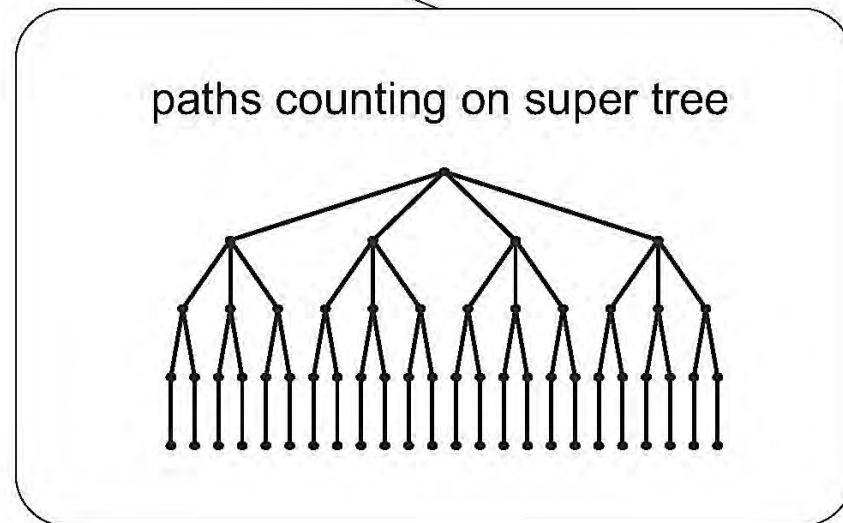
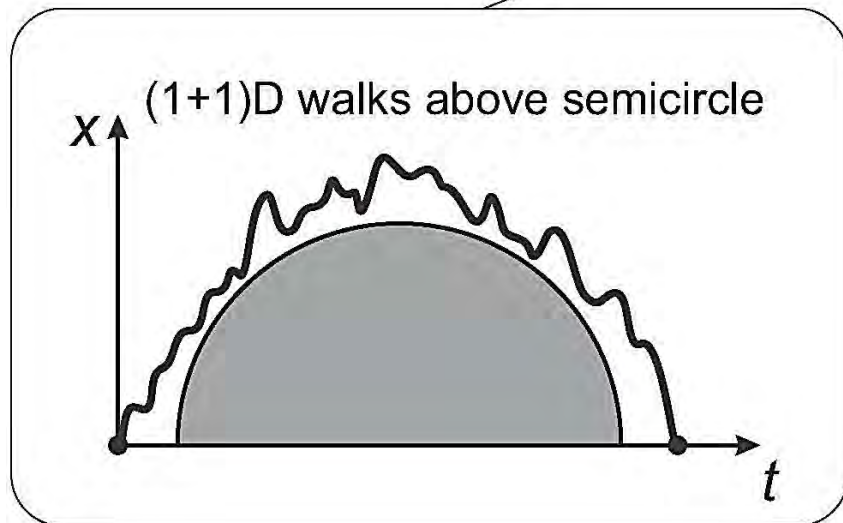
stretched paths
above triangle

$$\langle d \rangle = \text{const}$$

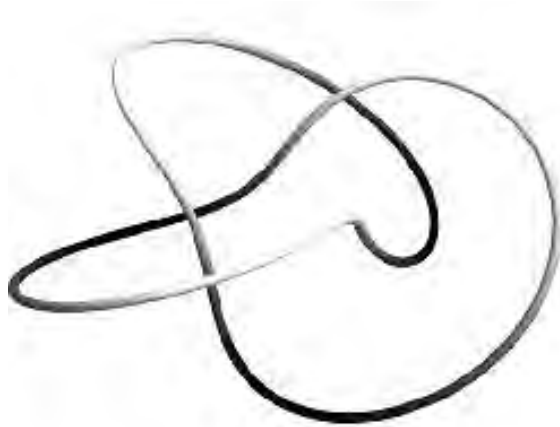
$$\langle d \rangle \sim R^{(\gamma-1)/(2\gamma-1)}$$



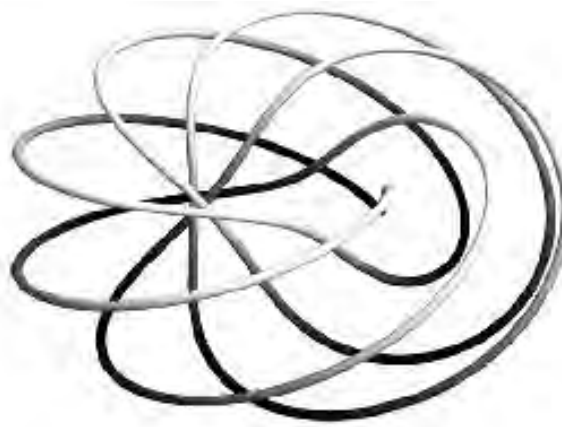
KPZ extremal statistics



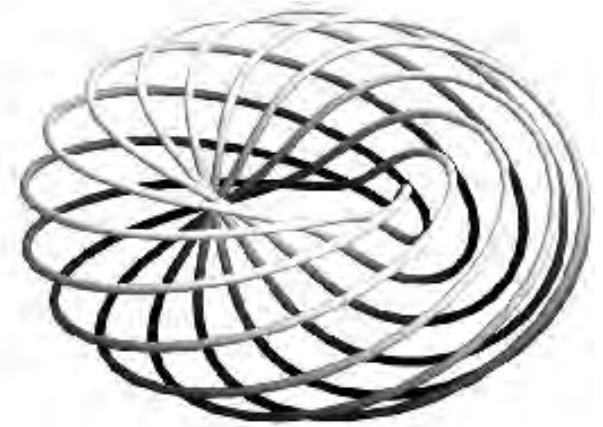
Torus knots



$T_{2,3}$



$T_{5,6}$



$T_{10,11}$

HOMFLY polynomial $\bar{P}(K)(q, a)$ satisfies skein relation

$$a\bar{P}\langle \begin{array}{c} \nearrow \\ \searrow \end{array} \rangle - a^{-1}\bar{P}\langle \begin{array}{c} \searrow \\ \nearrow \end{array} \rangle = (q - q^{-1})\bar{P}\langle \rangle \langle \rangle$$

Consider *reduced* HOMFLY $P(K)(q, a) = \frac{\bar{P}(K)(q, a)}{\bar{P}(unknot)}$

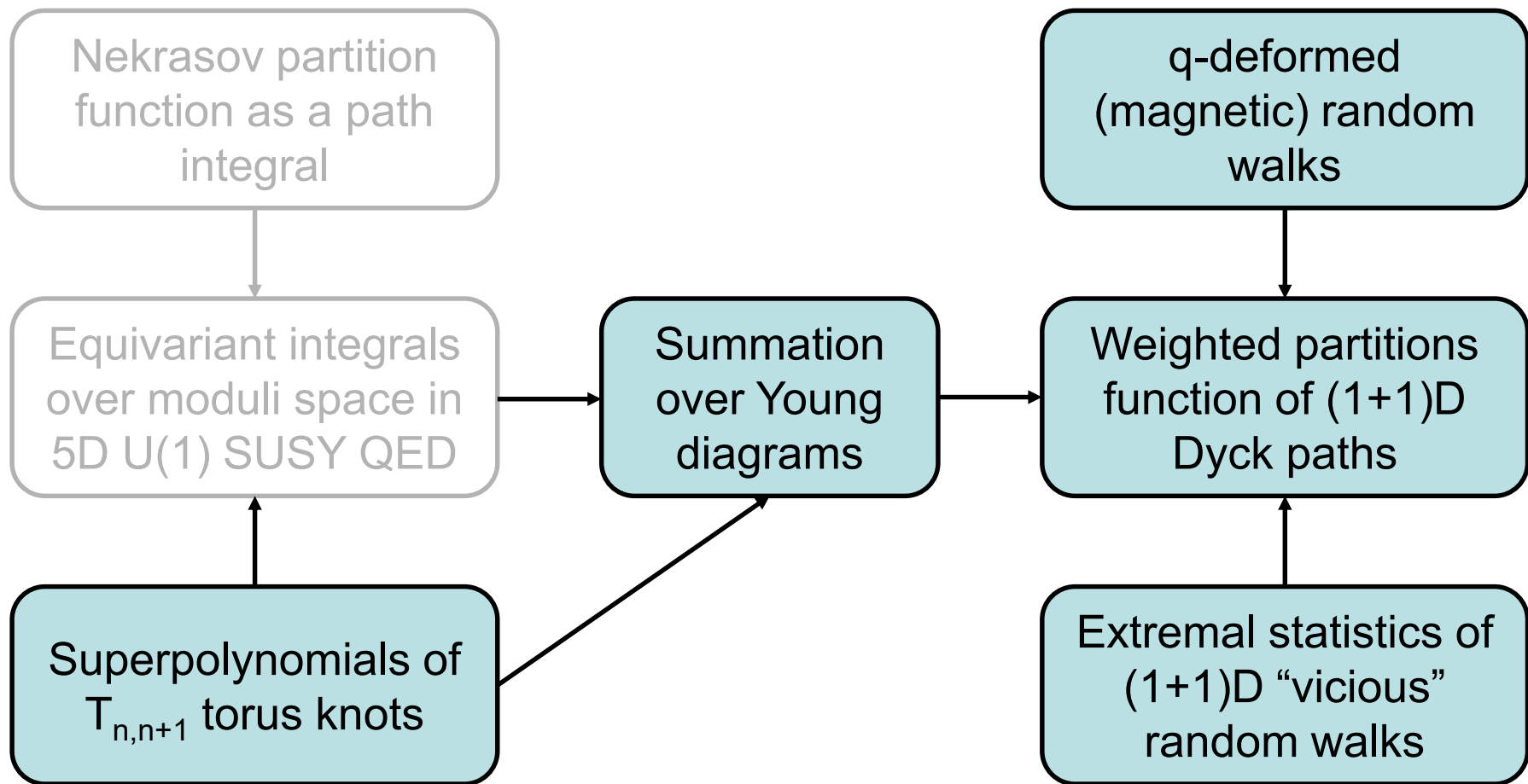
E. Gorsky (2011), and A. Oblomkov, J. Rasmussen, V. Shende and E. Gorsky (2012) showed that HOMFLY $P(K)(a, q)$ for $T(n, n+1)$ torus knots can be written as Narayana generating function

$$P_n(K)(q, a) = \sum_{\substack{\text{Dyck paths} \\ \text{of length } n}} a^{\text{corners}} q^{\text{area}}$$

Proof involved consideration of Euler characteristic of triply-graded knot homology $H_{i,j,k}$ in terms of Young diagrams

$$P(K)(q, a, t) = \sum_{i,j,k} a^i q^j t^k \dim H_{i,j,k}$$

$$P(K)(q, a, t = -1) \equiv P(K)(q, a)$$



K. Bulycheva, A. Gorsky, S.N. , Critical behavior in topological ensembles, 2015

Having connection between:
small-viscosity Burgers equation
area- and corner-weighted Brownian excursions
HOMFLY polynomials for $(n, n+1)$ torus knots
we may investigate and interpret the
critical behavior in knot ensembles

What is the physical meaning of singularities
in knot generating functions?

Conjecture:

Below and above the critical point the knot
discrimination is different